DEVELOPMENT OF THIN FILM FOR ALUMINIUM-AIR BATTERY

RYAN WONG KOK SENG

UNIVERSITI TUNKU ABDUL RAHMAN

DEVELOPMENT OF THIN FILM FOR ALUMINIUM-AIR BATTERY

RYAN WONG KOK SENG

A project report submitted in partial fulfilment of the requirements for the award of Bachelor of Mechanical Engineering with Honours

Lee Kong Chian Faculty of Engineering and Science
Universiti Tunku Abdul Rahman

October 2024

DECLARATION

I hereby declare that this project report is based on my original work expect for citations and quotations which have been duly acknowledged. I also declare that it has not been previously and concurrently submitted for any other degree or award at UTAR or other institutions.

Signature	:	*Ryan Wong*
Name	:	RYAN WONG KOK SENG
ID No.	:	20 UEB 06295
Date		2 October 2024

APPROVAL FOR SUBMISSION

I certify that this project report entitled **"DEVELOPMENT OF THIN FILM FOR ALUMINIUM-AIR BATTERY"** was prepared by **RYAN WONG KOK SENG** has met the required standard for submission in partial fulfilment of the requirements for the award of Bachelor of Mechanical Engineering with Honours at Universiti Tunku Abdul Rahman.

Approved by,

Signature	:	*WengCheong*
Supervisor	:	Dr. Tan Weng Cheong
Date	:	2 October 2024

ACKNOWLEDGEMENTS

I would like to express my sincere gratitude to my supervisor, Dr. Tan Weng Cheong for his patient guidance, valuable advices and moral supports throughout the entire project. The advices given were comprehensive and knowledgeable which helps me a lot in solving challenges during my research and completing my project.

In addition, I am also thankful to my beloved parents and supportive friends who constantly give me ancouragement on this research journey.

ABSTRACT

The advent of the Fourth Industrial Revolution (IR 4.0) drives a significant increase in energy demand, highlighting the limitations of fossil fuels and the urgent need for renewable energy and advance storage solutions. While Lithium-Ion batteries dominate the battery market, their toxic chemical content contributes to environmental pollution during production and disposal, highlighting the need for more sustainable practices and greener alternatives. Aluminium-air batteries (AABs) present a promising alternative due to their high energy density, specific capacity, and environmental advantages. However, AABs face challenges such as rapid anodic corrosion in alkaline solutions, significant hydrogen gas evolution, and electrolyte leakage. To address these issues and reduce environmental impact, this study explores the use of nanocellulose-incorporated gel electrolytes as a thin film for AABs. Various thin films cellulose gel electrolyte with differing thicknesses, nanocellulose content, and KOH concentrations were fabricated, and the electrochemical properties of AABs using these films were analysed. Furthermore, the Al-air battery incorporated with thin film cellulose gel electrolyte are subjected to battery performance analysis including polarization test, constant current discharge test, corrosion test, water absorption test, shrinkage test, reusability test and Scanning Electron Microscopy (SEM) Analysis. The results reveal that the incorporation of nanocellulose into gel electrolyte achieve an open circuit voltage (OCV) of 1.86 V and enhances the peak power density of Al-air battery to 91 mW as compared to 55 mW from the gel electrolyte without nanocellulose. The discharging time for the thin film cellulose gel electrolyte also improved significantly to 95 minutes with 10 mA of discharging current. Additionally, with the investigation of the effect of gel electrolyte thickness, effect of nanocellulose content and effect of potassium hydroxide concentration on the performance of Al-air battery, it reveals the thin film cellulose gel electrolyte with 10 wt% nanocellulose content, thickness of 20 ml content volume and 3 M of potassium hydroxide deliver the best performance among all the gel electrolyte fabricated. With an open circuit voltage (OCV) of 1.95 V, the battery was able to maintain a discharging period around 7 and half hours along with a peak power density of 187 mW.

TABLE OF CONTENTS

LIST OF FIGURES

LIST OF TABLES

LIST OF SYMBOLS / ABBREVIATIONS

IR 4.0	Industrial Revolution 4.0
EV	Electric Vehicles
AAB	Aluminium-air Battery
PVDF	Polyvinylidene Difluoride
PTFE	Polytetrafluoroethylene
OER	Oxygen Evolution Reaction
ORR	Oxygen Reduction Reaction
CNTs	Carbon Nanotubes
N-CNO	Nitrogen-Doped Carbon Nano Onion
PVA	Poly(vinyl) Alcohol
CNF	Cellulose Nanofiber
DMAc	N,N-Dimethylacetamide
NCC	Nanocellulose

CHAPTER 1

INTRODUCTION

1.1 General Introduction

With the approaching of Industrial Revolution (IR 4.0) necessitates significant energy usage, with a considerable demand for energy resources. However, eco-friendly alternative energy sources are widely emphasized concerning to the limitations of conventional energy sources including environmental pollution, global warming, depletion of fossil fuels. Furthermore, fossil fuels based energy is a non-renewable energy source and it will eventually deplete with the massive consumption leading to energy crisis. Energy is important as it is the fundamental resource on powering devices, hence, it is prudent to also discover safer, more reliable, and efficient energy storage solutions to be integrated into the IR4.0 applications. There are several renewable energy sources including hydropower energy, solar energy as well as wind energy that are explored to address the energy crisis issue. In addition to examining energy sources, it is important to also investigate solutions for storing energy. Among the energy storage solutions, batteries are commonly selected owning to their high energy density with satisfactory electronic efficiency making them applicable for portable electronic devices and large applications such as electric vehicles (EVs). Regarding to battery, Lithium-Ion batteries are commonly mentioned and have dominated the market. However, with the energy density of Li-ion battery having approximately 100~200 Wh/kg, the applications such as electric vehicles (EVs) requiring high energy and power density remain somewhat limited. (Liu, et al., 2017)

While numerous studies have focused on the improving the performance of Lithium-Ion Batteries, there is a need to explore alternative energy storage solutions. (Xia, et al., 2015) The metal-air batteries has gained considerable attention recently and considered to be a potential alternative among the energy storage solutions as it possess high energy density and capacity while maintain a discharge voltage along with minimal dependance of capacity on operating temperature. (Rahman, et al., 2013) Generally, metal-air batteries feature a metal anode and an air cathode to generate electrical energy through chemical

reaction when immersed in a suitable electrolyte. The design of metal-air batteries is able directly received oxygen from the surrounding allowing it to have high energy densities in a compact and light mass. Several studies were conducted to investigate and compare the characteristics of metal-air batteries using various common metal includes lithium (Li), magnesium (Mg), sodium (Na), zinc (Zn) and aluminium (Al).

According to the previous study, Li-air battery offers a theoretical energy density of 13 kWh/kg which is the highest among the metal choices, but it still has many challenges such as the instability of lithium under humid environments, blockage of carbon cathodes by the discharge products and side product formation during cycling affecting the reversible charging capability and overall cycle life. (Liu, et al., 2017) Conversely, Zn-air battery is rechargeable, but it has the lowest theoretical energy density of 1.3 kWh/kg providing a limited life cycle and suffer from dendrite formation along with high charge overpotentials. (Hardwick and Bruce, 2012) Similarly, the Mg-air batteries and Na-air batteries suffer low theoretical energy density with value of 1.6 kWh/kg and 6.8 kWh/kg respectively which affects the cycle life of the battery. However, Mg-air battery is not rechargeable, and it face the challenge of high corrosion rate contributing to short shelf life. (Yang, 2002) Conversely, Al-air battery experience the same hindrance as Mg-air battery being non-rechargeable, but it was reported that Al-air battery with ionic liquid solve the issue of rechargeability. Nonetheless, Al-air battery still gain interest in the energy storage system owning to its high theoretical specific capacity of 2.98 Ah/g, high theoretical voltage of 2.7 V and high theoretical energy density of 8.1 kWh/kg. (Nestoridi, et al., 2008) Moreover, aluminium is lightweighted and naturally abundant making it inexpensive, environmentally friendly, and high recyclability. Thus, this study will continue exploring the potentiality of Aluminium-air Battery (AAB) technology.

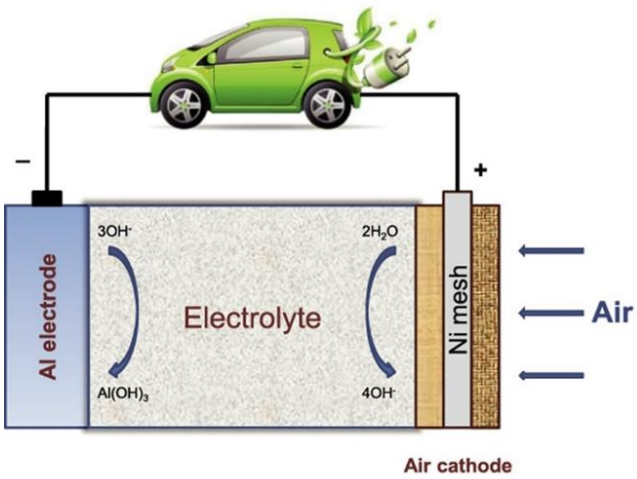

Figure 1.1: Schematic Illustration of Al-air Battery (Liu, et al., 2017). Copyright 2017. Elsevier.

1.2 Importance of the Study

The outcome of this present study may propose an alternative modification to the Al-air battery and solve challenges related to the anodic corrosion that led to low performance of the battery while providing an analysis on the Al-air battery fabricated using thin film cellulose gel electrolyte. There are many reviews on Al-air batteries that concentrates and reviewing on the key components of Al-air batteries which includes the anode, cathode, electrolyte, and design respectively. This study attempts to focus on the fabrication and evaluation of the thin film cellulose gel electrolyte incorporate in Al-air battery. The development of a gel electrolyte in Al-air batteries can potentially create several possibilities for various applications especially with the emergence of IR4.0 applications, flexible wearable device as well as the electric vehicles (EV) industry. The implementation of gel electrolyte in Aluminium-air batteries application generally features the ability to eliminate leakage issues while providing thermal and electrochemical stability. However, the current implementation of gel electrolyte in Al-air batteries is still not sufficient to apply in industrial usage and hindered by the problems associated with limited shelf life of the battery and low discharging performance. In this study, it is aspired that the thin film cellulose gel electrolyte can overcome the conventional design of Al-air batteries being bulky by reducing the complexity of the cell. Hence, it allows the possibility of practical applications such as wearable applications.

1.3 Problem Statement

Numerous research has assessed the performance of Al-air batteries indicating its potential to meet the future energy demands as a sustainable energy storage solution. Nonetheless, there are still problems associated with the Al-air battery including rapid anodic corrosion in alkaline solutions, significant hydrogen gas evolution as well as electrolyte leakage hindering the performance of the Al-air battery. The implementation of gel electrolyte provides a solution to the issues associated with the conventional Al-air battery. The gel electrolyte immersed in aqueous solution helps to reduce the anodic corrosion and mitigate the hydrogen gas evolution as it limits the electrolyte interaction on the Al surface. Furthermore, gel electrolyte can eliminate the concerns related to leakage while act as a separator for the cathode and anode to prevent short circuit. However, the conventional gel electrolyte is hindered by the challenges of low ionic conductivity and limited shelf life. The incorporation of nanocellulose into gel electrolyte offers high porous structure which can potentially limits the excessive electrolyte to interact with the Al anode and allow better electrolyte uptake ability resulting in better electrochemical properties of the Aluminium-air battery.

1.4 Aim and Objectives

The aim is to develop a thin film gel electrolyte incorporated with cellulose for Al-air battery and the specific objectives of this study are as follows:

i. To fabricate a thin film cellulose gel electrolyte for the Al-air battery.
ii. To investigate the influence of gel electrolyte with different thickness on the electrochemical properties of the Al-air battery.
iii. To investigate the influence of the concentration of potassium hydroxide in the thin film cellulose gel electrolyte on the electrochemical properties of the Al-air battery.
iv. To investigate the discharging performance and discharging capacity of thin film cellulose gel electrolyte in the Al-air battery.

1.5 Scope and Limitation of the Study

The scope of the study is to synthesize a thin film cellulose gel electrolyte and study the electrical performance including the discharging performance,

discharging capacity, and life cycle of the Aluminium-air battery. Despite gel electrolyte has gained popularity as an alternative to liquid electrolyte in Al-air batteries, there remains a scarcity of research and ongoing testing regarding the incorporation of binders and crosslinking agent into gel electrolyte, as well as the investigation of potassium hydroxide concentration within the gel electrolyte. Therefore, these aspects will also be addressed within the scope of this study. Nevertheless, the study's limitation is its exclusion of the investigation into the mechanical properties of thin film cellulose gel electrolytes. In addition, the gel electrolyte inherent the characteristic of swelling contributing to the limitation of the study. A potential limitation affecting this study is the duration for which gel electrolyte can be stored, as it is prone to degradation over time due to variables like temperature changes and exposure to air.

1.6 Contribution of Study

This study proposed the incorporation of nanocellulose in the fabrication of gel electrolyte and provided a novel approach on the performance of the Al-air battery using various gel electrolyte fabricated. The findings of this study may offer valuable insights for future advancements aimed at addressing the challenges of Al-air batteries, potentially improving their performance based on the outcomes obtained from the research.

1.7 Outline of Report

The overall report consists of 5 chapters which discuss on the performance of Al-air battery with thin film cellulose gel electrolyte. Chapter 1 Introduction mainly covers the background of the research topic, the problem statement, aim and objectives with the scope and limitations of the research. In addition, Chapter 2 Literature Review involved a detailed review on the Aluminium-air battery technology. Chapter 3 Methodology and Work Plan outlines the procedures and tests conducted whereas Chapter 4 presents the results and a detailed analysis. Finally, Chapter 5 Conclusion provides a summary and conclude any important findings as well as providing recommendations for future developments.

CHAPTER 2

LITERATURE REVIEW

2.1 Anode

2.1.1 Pure Aluminium

Pure Aluminium is consistently selected as the anodic material in metal-air batteries due to its advantageous characteristics including high energy density, negative charge potential, being able to recycle, naturally abundance, and excellent electrochemical properties. When compared to a Hg/HgO reference electrode, a pure Al anode exhibits a potential of -2.35 V in aqueous solution and -1.66 V in saline solution. (Parsons, 1967; Doche, et al., 1999) However, the actual open-circuit potential of the Al electrode tends to be elevated, mainly because of the competition among various electrode processes occurring on its surface. (Liu, et al., 2017) These processes encompass the initial formation of Al_2O_3 layer followed by $Al(OH)_3$ layer, the transfer of 3 electron charge process resulting in aluminium ion production, the development of corrosion products such as $Al(OH)_3$ and $Al(OH)_4^-$, and the occurrence of parasitic reactions on the aluminium surface leading to hydrogen evolution. (Mohamad, 2008; Bernard, et al., 2006) The parasitic reaction contributes to passivation and corrosion of the Al surface and can be represented in the equation, $2Al + 6H_2O \rightarrow 2Al(OH)_3 + 3H_2$. This will tentatively lead to low performance of the Al-air batteries. (Doche, et al., 1999) Despite that these processes elevates the open-circuit potential of the aluminium electrode, they ultimately present as challenge for Al-air batteries and eventually leading to failure of it.

The common problem associated with aluminium being the anodic material of metal-air batteries is the instantaneous development of a naturally occurring oxide layer on the aluminium surface when in contact with air and aqueous solution. The surface passivation increases the corrosion rate of the aluminium electrode and significantly affects the rate of aluminium activation. The self-corrosion at the Al electrode discourages storage of Al-air batteries in wet environments and adversely affects the capacity of the batteries along with the reduction of discharge efficiency. (Egan, et al., 2013) Recently, there are studies conducted by selecting the 2N5 commercial grade aluminium (99.5%

purity) and 4N high pure grade aluminium (99.99% purity) as the anodic material. The use of 2N5 commercial grade aluminium in aluminium-air batteries results in lower performance compared to 4N high pure grade aluminium due to inherent impurities and the formation of an impurity complex layer. It decreases battery voltage during standby status, reduces discharge current, and diminishes the efficiency of the battery at the standard operating voltage of 1.0 V for Al-air batteries. Nonetheless, the impurity complex layer in 2N5 grade aluminium dissolves as the discharge voltage decreases to 0.8 V. The dissolution improves the discharge current density and efficiency of the battery by minimizing the self-corrosion reaction. Hence, there are research suggest the potential use of 2N5 grade aluminium as the anodic material given it is economical. (Cho, et al., 2015) Overall, pure aluminium is infeasible and impractical in the application of Al-air batteries as it suffers from rapid corrosion rate and parasitic reaction which leads to hydrogen evolution on the surface when feature as the anodic material in the battery.

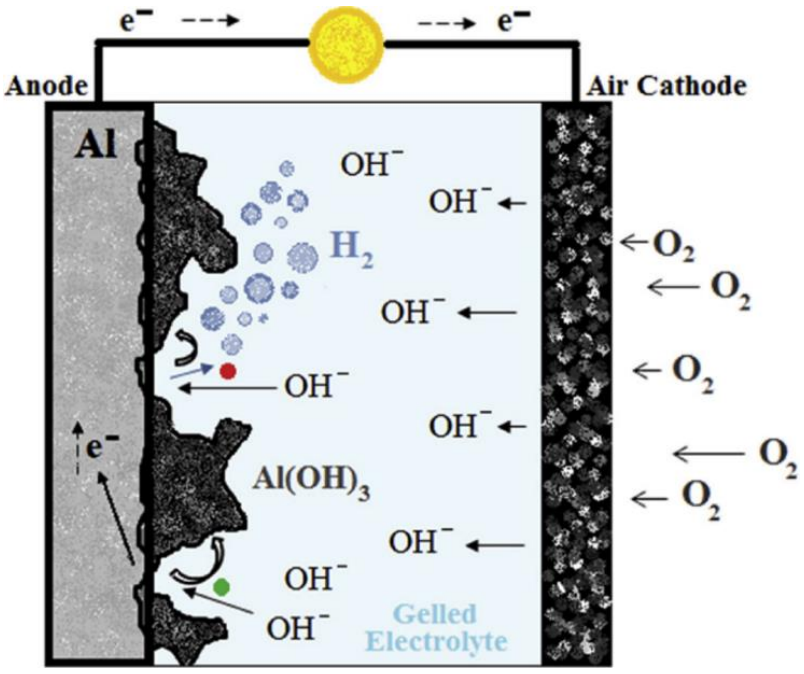

Figure 2.1: Schematic Illustration of Aluminium Self-corrosion and Oxidation Process in Al-air Battery (Pino, et al., 2015). Copyright 2015. Elsevier.

2.1.2 Aluminium Alloys

Pure aluminium is rather infeasible when selected as anodic material in Al-air battery as it corrodes rapidly and occurs parasitic hydrogen evolution when introduced to aqueous electrolyte. Hence, alloying aluminium has been studied to eliminate the limitations associated with pure aluminium to prolong the battery operation time and serves as an alternative in the anodic material of Al-air batteries. There are various elements including Ti, In, Ga, Zn, Sn, Bi, Mg and Mn that were incorporated as alloying elements for composition of aluminium alloys. Among the adopted elements gallium (Ga), zinc (Zn), indium (In), and tin (Sn) are commonly used as doping element for aluminium alloys as they offer different advantage to the Al-air battery. Thus, combining each of these alloying elements contribute to the exceptional performance of aluminium alloys in Al-air batteries.

Zinc (Zn) is claimed to be popular for reducing the parasitic reaction of hydrogen evolution on Al anode through the increase of hydrogen evolution potential in addition to the relieving of the Al anode degradation. (Pino, et al., 2015) However, Al-Zn showed a shorter voltage stabilization time when comparing with pure 4N Al. Throughout the research, the content of aluminium used for the alloy is 99.75% doped with iron (Fe) and tin (Sn) as opposed to commonly used aluminium with content of 99.99%. As a result, the corrosion reduction caused by Zn is dominated by the corrosion from Fe and Sn. (Park, et al., 2017) In addition, it is found that Al-Zn alloys forms oxidation layers includes type 1, which consists of porous $Zn(OH)_2$ and defective ZnO, and type 2, which consists of protective layer ZnO. The discharging performance of the battery significantly decreased by the presence of the protective ZnO layer, but it can be reduced by doping indium (In) into the Al-Zn alloy resulting in Al-Zn-In alloy as it impedes the protective ZnO layer formation. Additionally, a study was conducted to investigate and compare the performances of Al-air batteries with pure Al and Al-0.5In (wt%) selected as anodic material in a 4 M NaOH solution.

Generally, indium (In) is proven to be advantageous as an alloying element in the composition of Al alloys as it exhibits high anodic efficiency and increases the hydrogen evolution potential. (Sun and Lu, 2015) The results indicates that the Al-In alloy exhibit higher anodic efficiency due to lower self-

corrosion rate compared to pure Al leading to higher capacity. On the other hand, introducing gallium (Ga) as an alloying element in the composition for Al alloys limits the passivation of Al_2O_3 oxide layer and increases the aluminium diffusion and dissolution by breaking down and thinning the oxide layer. (Sun, et al., 2015; Tuck, et al., 1987) Furthermore, tin (Sn) when doped in the composition of Al alloys drive the activating behavior relative to aluminium thereby increases the dissolution rate of Al in the battery with minimal corrosion behavior. The anodic dissolution decreases noticeably when approaching higher potentials. (Sun, et al., 2015; Lee and Kim, 2001)

As each individual alloying element retain certain advantage when doped with aluminium as Al alloy, there have been studies conducted to combine the alloying element. The Al-1Mg-1Zn-0.1Ga-0.1Sn (wt%) and Al-1Mg-0.1Ga-0.1Sn (wt%) alloys were selected as the anode for the Al-air batteries and studied thoroughly. Generally, the alloy containing Zn perform better in terms of the electrochemical performance with lesser anodic degradation. (Ma, et al., 2014) Furthermore, Wang et al. (2017) proposed a selection on Al-0.15Bi-0.15Pb-0.035Ga (wt%) alloy as the anodic material which possess a satisfactory result having nearly 2 times of peak power density, 253.4 ± 2.5 mW/cm^2 comparing with pure aluminium, 108.5 ± 2.5 mW/cm^2 when immersed in KOH solution. It also shows a higher anodic efficiency 85.40 ± 5 % comparing with 73.6 ± 1.0 % by pure aluminium. Due to the presence of Bi, PB and Ga, the hydrogen evolution potential increases leading to lower rate of corrosion for the alloy. (Wang, et al., 2017) As of current, the Cu-deposited 7075 T-7351 Al alloy with wt% of 5.6-6.1 Zn, 2.1-2.5 Mg, 1.2-1.6 Cu, < 0.5 Si, Fe, Mn, Ti, and Cr arguably the preferred alloy for the composition of Al alloy as it shows the most convincing results. The homogenous absorbed layer of Cu that is electrochemically formed creates a solution to the challenges related to the hydrogen evolution by developing a barrier which reduces the hydrogen evolution rate while maintaining the Al efficiency as the anode. Due to the nature of copper, when include in the Al alloys, the discharging performance, and the battery potential increases significantly with minimal anodic resistance. (Mutlu and Yazıcı, 2018) Substantially, doping elements in composition of Al alloy create a solution to the hindrance of self-corrosion rate in the anode and

hydrogen evolution but requires a relatively higher cost as compared to pure Al depending on the choice of fabrication process and the elements involved.

2.2 Air Cathode

The Al-air batteries feature an air-breathing cathode otherwise known as the air cathode, and it is crucial for completing the electrochemical process within the battery. The air cathode is made up of a current collector , gas diffusion layer, and a catalytic active layer. The gas diffusion layer is constructed from a carbon material and a hydrophobic binder including polyvinylidene difluoride (PVDF) or polytetrafluoroethylene (PTFE). The presence of the binder film is used to ensure only the permeation of air instead of water or electrolyte. (Harting et al., 2011), (Li, et al., 2016) The current collector is usually constructed from a mesh made of nickel (Ni) which provides structural reinforcement to the cell while facilitates and enhances the electron transfer process. (Liu, et al., 2017) The impracticality of Al-air batteries applications is contributed by the slow oxygen reduction reaction (ORR) and oxygen evolution reaction (OER) which primarily occur at the catalytic active layer that comprises of an electrocatalyst, carbon materials and binder.

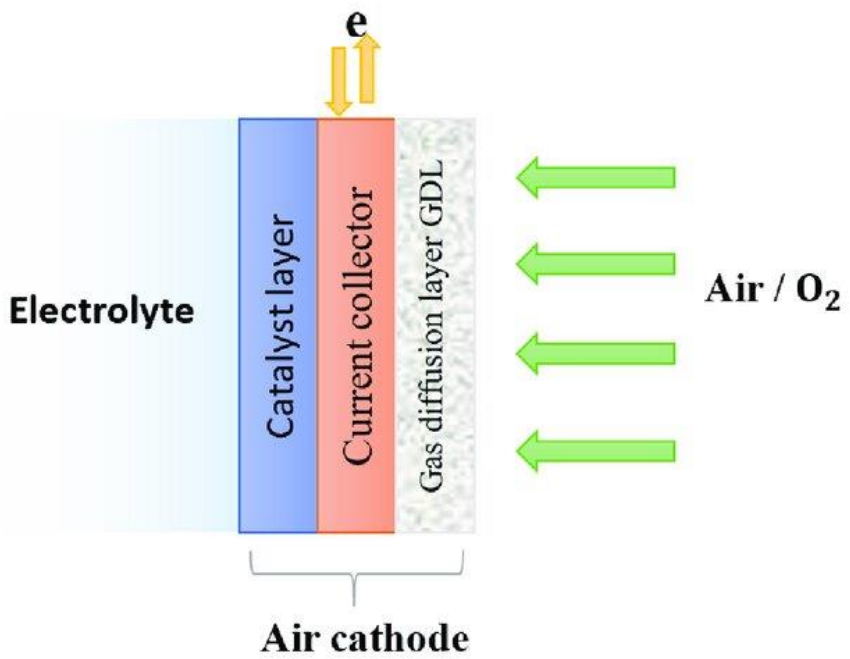

Figure 2.2: Schematic Illustration of Air Cathode (Olabi, et al., 2021). Copyright 2021. Creative Commons.

2.2.1 Oxygen Reduction Reaction (ORR)

The oxygen reduction reaction (ORR) primarily occurs by reducing the oxygen molecule in an aqueous alkaline electrolyte following both the direct four-electron pathway and the successive two-electron pathway. Among these, the direct four-electron pathway is more preferrable in the oxygen reduction reaction and represented in equation (2-1). On the other hand, the successive two-electron pathway expressed in equations (2-2), (2-3) and (2-4) experiences an initial reduction to peroxide HO_2^- and following with a two-electron reduction from HO_2^- to OH^-. However, when the reactions in equation (2-2) and (2-3) occurs rapidly, the ORR is likely to happen through the four-electron pathway. On the contrary, the direct four-electron pathway and the successive two-electron pathway in acidic solution is represented in equations (2-5), (2-6), (2-7) and (2-8). (Li and Chen, 2013)

Equation for the direct four-electron pathway in alkaline medium:

$$O_2 + 2H_2O + 4e^- \rightarrow 4OH^- \qquad E^0 = 0.401 \text{ V vs. SHE} \qquad (2\text{-}1)$$

Equations for the successive two-electron pathway in alkaline medium:

$$O_2 + H_2O + 2e^- \rightarrow HO_2^- + OH^- \qquad E^0 = -0.076 \text{ V vs. SHE} \qquad (2\text{-}2)$$

$$HO_2^- + H_2O + 2e^- \rightarrow 3OH^- \qquad E^0 = 0.878 \text{ V vs. SHE} \qquad (2\text{-}3)$$

$$HO_2^- \rightarrow 2OH^- + O_2 \qquad (2\text{-}4)$$

Equation for the direct four-electron pathway in acidic medium:

$$O_2 + 4H^+ + 4e^- \rightarrow 2H_2O \qquad E^0 = 1.229 \text{ V vs. SHE} \qquad (2\text{-}5)$$

Equations for the successive two-electron pathway in acidic medium:

$$O_2 + 2H^+ + 2e^- \rightarrow H_2O_2 \qquad E^0 = 0.695 \text{ V vs. SHE} \qquad (2\text{-}6)$$

$$H_2O_2 + 2H^+ + 2e^- \rightarrow 2H_2O \qquad E^0 = 0.878\ \text{V vs. SHE} \qquad (2\text{-}7)$$

$$2H_2O_2 \rightarrow 2H_2O + O_2 \qquad (2\text{-}8)$$

2.2.2 Catalysts

The electrocatalyst in the catalytic active layer of the air cathode significantly influences the performance of the electrode and the energy density. Generally, the cathodic material should incorporate with suitable electrocatalyst to improve the oxygen reduction reaction (ORR) efficiency, the formation of by-products and improve the rate of electrode kinetics. There has been various selection of electrocatalytic materials used as the cathodic catalysts which includes noble metals & alloys, carbonaceous materials, transition metal oxides, polymer, and polymer-based complexes. However, in this research will only covers the noble metals and alloys as well as the carbonaceous materials along with transition metal oxides.

2.2.2.1 Noble Metals & Alloys

Gold (Au), silver (Ag), palladium (Pd) and platinum (Pt) are usually the preferred noble metal catalysts as they offer an unoccupied d-orbital providing vacancy for the reactant molecules which allows the occurrence of catalytic activity. The catalytic activity of noble metals is generally defined by their surface atomic configuration and electron level state. Hence, through the modification of the surface atomic configuration, the catalytic activity performance of noble metal catalysts can be improved in a positive way. This fairly explains the widely usage of platinum (Pt) as catalysts in the application of batteries. As of the current, the Pt-based catalysts which involves platinum nanoparticles supported by a carbon framework enhances the surface atomic configuration providing high electrocatalytic activity, stability and is known to be the state-of-the-art ORR electrocatalyst. (Wang, et al., 2008) While numerous research suggest that catalytic activity is primarily influenced by the particle size, it is also worth mentioning that the crystallographic facets impact on the catalytic activity within the air cathode. (Ge, et al., 2015) However, the high cost of Pt-only catalysts making it inadequate as a selection. Thus, Pt-metal alloys which surprisingly offer better catalytic activity performance are

introduced as a substation for Pt-only catalysts. The Pt lattice parameter is reduced through the incorporation of transition metal with small-size atoms into the Pt lattice. Furthermore, the differences in the electronegativities within the Pt-metal alloy system altered the transfer of charge from the transition metal to Pt during the filling of Pt d-orbitals. Howbeit, alloying Pt with suitable transition metals come with a cost of more complicated synthesis process and preparation. (Wang, et al., 2008)

2.2.2.2 Carbonaceous Materials

Among the choices for the selection of catalysts, carbonaceous materials are the preferrable ones as they have been consistently providing satisfactory catalytic activity and durability towards the oxygen reduction reaction (ORR). These carbonaceous materials cost relatively lesser as compared to the noble metal catalysts, Pt and Ag while being able to have wide stabilization potential windows as well as superior electronic conductivity. Fundamentally, carbonaceous materials exist in diverse structural forms which covers Zero-dimensional (0D) fullerene, one-dimensional (1D) carbon nanotubes and nanofibers, two-dimensional (2D) graphene and graphite nanosheets or three-dimensional (3D) nanostructured carbon materials. Other structural forms of metals, metal oxides such as spinel and perovskite, metal nitrides, carbon and non-metals.

There are studies proven the viability of lower cost catalysts becoming a reliable alternative as to the commercial Pt/C catalysts. The analysis of a bifunctional Co-N/CN catalyst (at 800 °C) exhibits an onset potential of 0.987 V and prefer the direct four-electron pathway for the oxygen reduction reaction (ORR). Additionally, the oxygen evolution reaction (OER) shows an improvement being the onset potential of 0.98 V is relatively close to the potential of commercial Pt/C catalysts, 1.06 V and having similar current densities. (Shen, et al., 2018) Furthermore, the encapsulating iron (Fe) in the carbon nanotubes (CNTs) lessens the energy required to remove an electron from the surface of carbon which eventually improves the ORR activity. It can be further improved with nitrogen (N) doping. (Deng, et al., 2012; Mamtani, et al., 2018; Liu, et al., 2016) It was discovered that most catalytically CNTs for ORR activity are the ultra-thin CNTs doped with high concentration of nitrogen

(N). As compared to the commercially available Pt/C catalysts, the CNTs doped with nitrogen (N) and encapsulated within ferric carbide nanoparticles (Fe_3C) and pyrolyzed at 800 °C performs better showing remarkable onset potential of 0.098 V when measured against Ag/AgCl. (Zhong, et al., 2015) However, the synthesis method involved requires massive consumption of energy, hence, more environmentally friendly approaches for the catalyst synthetization are discovered. For instance, the nitrogen-doped carbon nano onion (N-CNO) developed using biomass collagen are reported to have satisfactory performance with improved onset potential and high current densities along with durability which is comparable to commercially available Pt/C catalysts. (Chatterjee, et al., 2018)

2.2.2.3 Transition Metal Oxide

On the other hand, transition metal oxides are widely explored as an alternative for the usage of conventional noble catalysts as it being naturally abundant, eco-friendly, inexpensive. The transition metal elements such as iron (Fe), cobalt (Co), manganese (Mn), and nickel (Ni) can exhibit in various oxidation states as it consists of multiple valences. (Byon, et al., 2011) However, only the transition metal, Mn will be covered in this section. Due to the multiple valence state of Mn, it exists in various oxidation states from +2 to +7. Therefore, it serves as an effective component for acting as a bifunctional catalyst and has been demonstrated to exhibit electrocatalytic capabilities for ORR under alkaline conditions. (Cheng, et al., 2009) Despite the valence state and elemental composition are same for the manganese oxides, the catalytic activity is significantly influenced by the crystallographic structures. (Cao, et al., 2003) Based on the past research conducted, MnO_2 have been proven to be satisfactory when selecting as the catalyst for ORR, but it is often associated with carbon for support due to MnO_2 offer low conductivity. (Roche, et al., 2006) Nonetheless, the electrocatalytic activities presented with MnO_2 are excellent.

2.3 Electrolytes

The electrolyte is an essential component within the Al-air battery as it is a conductive medium that facilitates ion transfer from the cathode to the anode. The parasitic reaction which leads to hydrogen evolution, precipitation reactions and the self-corrosion rate which happens at the aluminium anode were primarily influenced by the choice of electrolyte. It also significantly influences the overall potential and performance of the battery cell. Addressing the major problem associated with the Al-air batteries, several research were attempted to focus on the various form of electrolyte to suppress the unwanted effects occur in the cell. These includes aqueous alkaline electrolytes, salt electrolytes and acidic electrolytes with pH value of $7 < pH \leq 14$, $pH = 7$ and $1 \leq pH < 7$ respectively. Among these various form of electrolytes, aqueous alkaline electrolyte has been proven to perform the best as the electrolyte choice for the Al-air battery. Generally, alkaline electrolytes including aqueous sodium hydroxide (NaOH) and potassium hydroxide (KOH) are the preferred ones owning to their high ionic conductivity, non-toxicity, low viscosity, low overpotential, and rapid reaction kinetics. (Santos, et al., 2013; Mokhtar, et al., 2015) Hence, alkaline electrolyte is mainly discussed in this paper.

There have been studies investigating the anodic corrosion rate in KOH and NaOH using various methods such as weight loss technique, steady state technique and polarization technique. As adopting different kind of anodic materials in the alkaline electrolyte shows different characteristics of the cell. The corrosion dissolution of pure Al was analyzed with steady-state technique, it was revealed that pure Al remains in passive state as indicate in the delineated polarization curves. In addition to that, one of the studies investigating fine structured Al as anodic material in alkaline electrolytes for the AAB. It was reported that the Al anode with finer grain sizes enhances the performance of the battery in 4 M of KOH and NaOH due to the active dissolution. (Fan, et al., 2015)

Conversely, the efficacy of alkaline solutions as the choice of electrolytes significantly excels with Al alloys as anodic material. It was reported that incorporating In, Mg, Sn, and Ga into the composite of Al alloy improves the self-corrosion rate when immersing in 4 M NaOH. Furthermore, there are research revealing the integration of active metal into Al anode improves the

corrosion resistance leading to higher discharging capacity. (Wilhelmsen, et al., 1991) However, varying the operating temperature and KOH concentration significantly influences the polarization characteristics but doesn't affect on the mass transfer. (Chu and Savinell, 1991) Composite of Al alloy containing Al-Zn-Mg and Al-Zn-In were tested in 4 M NaOH at room temperature and reveal potentials of -1.67 V and -1.65 V respectively. Both composites suffer crystallographic pitting corrosion, in addition to that, Al-Zn-Mg alloys also undergo hemispherical pitting corrosion. However, the chemical dissolution by OH^- leads to significant anodic corrosion in both alloys. (Ma, et al., 2013) Addressing to the parasitic hydrogen evolution at the anode, past research has improvised a hybrid concept involving ordinary kitchen aluminium foil as anodic material, a H_2/air fuel cell and concentrated NaOH electrolyte shows significant improvement of power output with no sacrifice on the efficiency of the AAB. The research concludes that increasing the concentration of the alkaline electrolyte allows more power density but the self-corrosion at the anode remain significant. (Wang, et al., 2013) Generally, alkaline electrolytes offer high ionic conductivity with efficient oxygen reduction rates but often relates to various problems including rapid anode corrosion, potential leakage, significant hydrogen gas evolution.

2.4 Alkaline Based Gel Electrolyte

As liquid electrolytes pose various challenges such as rapid anode corrosion, leakage of electrolyte and significant hydrogen gas evolution, a considerable amount of research has been conducted to address these challenges. (Zuo, et al., 2020) One of the notable approaches being the advancement of gel-based electrolyte as it proposes an effective substitution to the aqueous electrolyte and solid-state electrolyte owning to its high ionic conductivity along with thermal and electrochemical stability while eliminating concerns related to electrolyte leakage extending the service life of Al-air battery. (Nada, et al., 2023; Guisao, et al., 2015) Gel electrolyte generally is neither solid nor liquid but comprises both the cohesive properties of solids and diffusive properties of liquids.

As of current, poly (vinyl alcohol) (PVA) has been utilized extensively as the polymer host in the gel polymer electrolytes comparing with other polymer due to its flexibility, good adhesion, and hydrophilicity as an

electrolyte reservoir. (Santos, et al., 2019) There are numerous studies utilizing PVA doped with potassium hydroxide (KOH) to feature in different electrochemical applications including super-capacitors and metal-air batteries. Incorporation of KOH into PVA was reported to promote the mobility of free ions inside the gel electrolyte film and produces high ionic conductivity of 4.7 $\times 10^{-2}$ S.cm^{-1}. (Yang and Lin, 2002) The ionic conductivity of PVA-KOH gel electrolyte strongly depends on the content of KOH ad H_2O within the film. Hence, indicating the importance of optimized concentration of the alkaline gel electrolyte. (Lewandowski, 2000; Yang and Lin, 2002) A stretchable flexible Zinc-Air battery is prepared by utilizing PVA-KOH based gel electrolyte which kept stable for up to 20 cycles but the system prepared exhibits significant defects being the dense cross-linking of PVA and the presence of surface water-resistant groups. These defects result in decreased KOH concentration and ion conductivity in gel electrolyte (10^{-4} ~ 10^{-3} S.cm^{-1}) (Qu et al.,2017). Other than that, a study suggested on the preparation of a gel electrolyte using potassium alcohol (PVA) reveals high ionic conductivity and electrochemical properties. (Ma, et al., 2014) However, the partial exposure and volatility of KOH causes water evaporation within the gel electrolyte leading to swelling effect whereas PVA tends to experience hardening from high concentration of alkaline. (Tran, et al., 2019; Fan, et al., 2019)

2.5 Cellulose

Recently, biodegradable matrixes obtained through natural renewable sources such as cellulose have attracted significant attraction in the field of gel electrolyte. Cellulose is a naturally abundant biomass material with macromolecule offering renewability, cost-effectiveness, eco-friendly nature along with inherent biocompatibility and biodegradability. Owning to its large number of polar hydroxyl groups consists of linear chains of repeating β (1→4) linked D-glucose units, it provides strong intramolecular and intermolecular hydrogen bond which result in superior thermal stability and mechanical property. (Moon, et al., 2011; Wang, et al., 2016; Chang and Zhang, 2011) Nanocellulose is a structural polysaccharide which formed from cellulosic extraction that have nano-scale structural dimensions. As the nanocellulose are extracted from plant, there are several options with different properties available.

Generally, the nanocellulose derived from coniferous plant otherwise known as the softwood have higher crystallinity and mechanical strength. There was a research suggesting the microparticles of the nanocellulose extracted from pine wood and corncob both have high crystallinity index of 67.8% and 70.9% respectively using spray-dying. (Ditzel et al., 2017) Another research has reported the extraction of nanocellulose from pine tree through delignification and bleaching process using different concentrations of acetic acid. The nanocellulose extracted with 10% of acetic acid is able to produce a crystallinity index of 55.60% with a width of 12.82 nm and length of 290.82 nm. (Aisiyah et al., 2020) Furthermore, a research provided a review on the strength and stiffness of the nanocellulose derived from softwood and describes the structure and the mechanical performance. With that being said, the nanocellulose derived from coniferous plant comes with high crystallinity and mechanical strength making it favourable for the application in gel electrolyte. (Aisiyah et al., 2020)

There was a report suggested a soy protein isolate/poly(vinyl alcohol) composite membrane was fabricated as a separator for lithium-ion battery reveals superior ionic conductivity of 3.8×10^{-3} $S.cm^{-1}$ along with good electrochemical stability. (Zhu, et al., 2016) Furthermore, research was conducted with cellulose nanofiber (CNF) as the derivative material to form a cellulose based separator. The results show that the cellulosic separator experience lesser meltdown when exposed to heat by overcharging of the lithium-ion batteries. (Kuribayashi, 1996) In addition, a composite membrane made of cellulose/polysulfonamide was developed and tested in lithium-ion batteries. The separator yields high thermal stability along with stable charging-discharging performance when operating at 120 ºC. Other than lithium-ion batteries, there is research applying thin film cellulose gel electrolyte for application of metal-air batteries. For instance, an Al-air battery was developed with cellulose paper as electrolyte substrate to substitute the circulation of electrolyte. It reveals that these cellulose paper separators act as corrosion inhibitors suppressing the self-corrosion at the Al anode while achieving satisfactory performance of open circuit voltage with a value of 1.6 V along with 21 mW/cm^2 peak density. The discharging capacity of Al-air battery shows a result of 1273 mAh/g when using NaOH as the electrolyte. (Wang, et al., 2019)

Aside from that, a water hyacinth cellulose nanofibrils was fabricated and uses as the separator in the Al-air batteries. It was further modified by incorporating a separator made of water hyacinth cellulose nanofibrils and polyethylene glycol in the ratio of 85 wt% and 15 wt%. The tested result from the research discloses that Al-air battery with the cellulose separator has a total discharge time of 307.85 min when using 10 mA of discharge current which performs better than the commercial filter paper as a separator. (Selan, et al., 2023) On top of that, a PVA-based cellulose composite hydrogel electrolyte was developed using carboxyl modified nanocellulose (C-CNFs) and tested in Zinc-air battery. The thermal stability and mechanical properties of the composite HGE improved significantly leading to extended cycle life and enhanced discharge capacity for the Zinc-air battery. (Li, et al., 2021) Overall, cellulose is a good separator especially incorporated in gel electrolyte.

2.6 Summary

Generally, aqueous alkaline electrolyte has the highest performance among all the electrolytes of choices but tends to suffer from rapid anodic corrosion and hydrogen evolution reaction. There have been several studies suggesting solutions to address the related problems. One of the notable approaches being the implementation of gel electrolyte as it acts as a good corrosion inhibitor. However, due to the hydrophobic properties of gel electrolyte making it have limited electrolyte uptake ability. Cellulose on the other hand fulfilled the characteristics as a good separator owing to its hydrophilic property which can retain the electrolyte. In this study, research is performed which incorporates cellulose into gel electrolyte developing a cellulose-based alkaline gel electrolyte.

CHAPTER 3

METHODOLOGY AND WORK PLAN

3.1 Overall Process Flow Chart

The Figure 3.1 below presents the overall process flow chart for this research project.

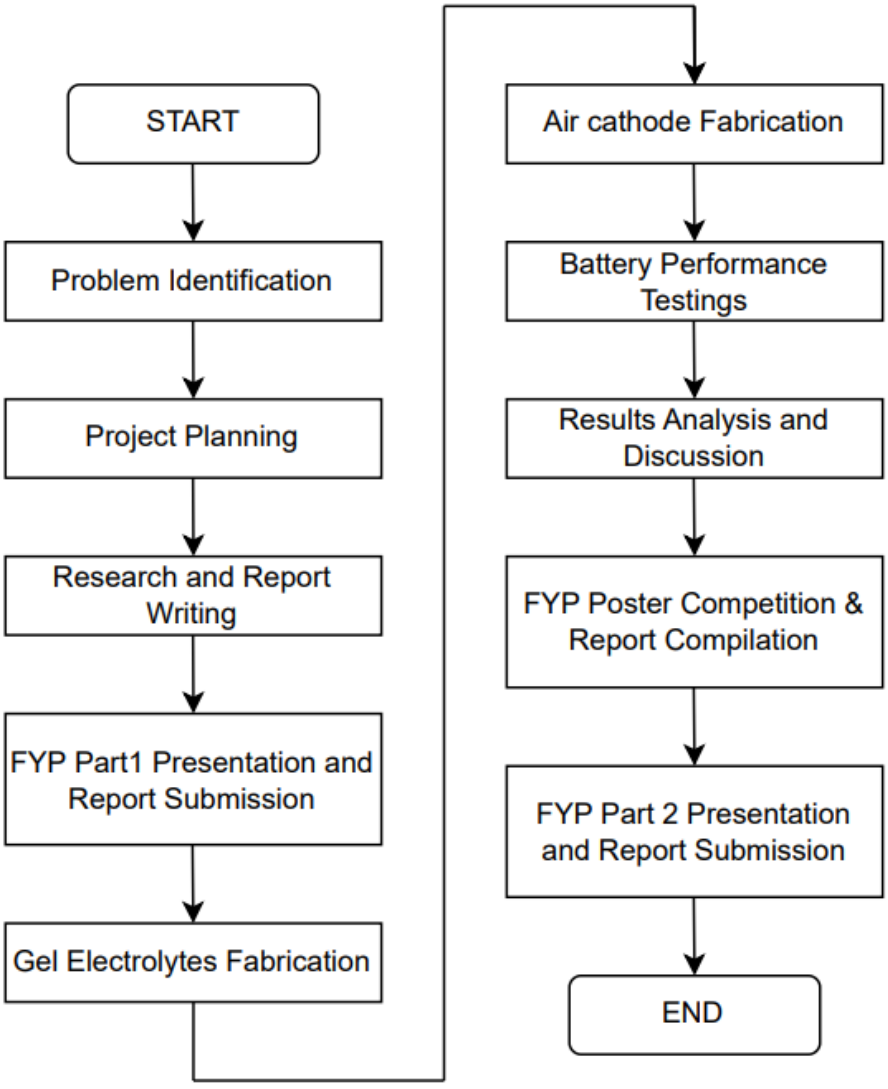

Figure 3.1: Overall Process Flow Chart.

3.2 Electrochemical Reaction

The usual electrochemical reactions in the Al-air batteries are represented by equation 3-1, 3-2 and 3-3 while the parasitic reaction which contributes to corrosion and passivation of Al anode is represented by equation 3-4.

The electrochemical reactions involved in the AAB are presented in these equations:

Anode: $Al \rightarrow Al^{3+} + 3e^{-}$ (3-1)

Cathode: $O_2 + 2H_2O + 4e^{-} \rightarrow 4OH^{-}$ (3-2)

Overall: $4Al + 3O_2 + 6H_2O \rightarrow 4Al(OH)_3$ (3-3)

Parasitic Reaction: $Al + 3H_2O \rightarrow Al(OH)_3 + 3/2H_2$ (3-4)

3.3 Preparation of PVA/KOH Alkaline Gel Electrolyte

A 10 wt% of Polyvinyl Alcohol (PVA) is prepared by mixing 10 g of PVA powder into 10 ml of distilled water using a magnetic stirrer for 1 hour at the temperature of 80 °C until a clear PVA solution is obtained. Next, 1 M of Potassium Hydroxide (KOH) alkaline solution is prepared by mixing the KOH pellets into the distilled water. After that, the KOH solution is added into the PVA solution and stirred for 1 hour using magnetic stirrer at ambient temperature. Subsequently, the PVA/KOH solution is poured into a petri dish and kept in vacuum condition to allow the removal of bubbles. Following that, the PVA/KOH solution is subject to freeze-thawing for 1 day and a gel electrolyte is formed. Finally, the gel electrolyte formed is then immersed into 1 M of KOH solution.

3.4 Preparation of PVA/KOH/Nanocellulose Alkaline Gel Electrolyte

To allow the dissolution of nanocellulose, a mixture solution comprising Sodium Hydroxide (NaOH) and Urea is first prepared at the ratio of 7 wt% to 12 wt%. It is then kept in the freezer for 1 hour. Subsequently, 10 wt% of nanocellulose (NCC) is added into the mixture solution and stirred continuously until the nanocellulose is completely dissolved. The NCC solution is then added

into 10 wt% of PVA and stirred continuously for 1 hour using magnetic stirrer at ambient temperature, thus forming a PVA/NCC solution. Next, 1 M of Potassium Hydroxide (KOH) alkaline solution is prepared by mixing the KOH pellets into the distilled water. Following that, the KOH solution is mixed with the PVA/NCC solution and stirred continuously for 1 hour at ambient temperature. After that, the PVA/NCC/KOH solution is poured into a petri dish and kept in vacuum condition kept in vacuum condition to allow the removal of bubbles. The PVA/NCC/KOH solution is then subject to freeze-thawing for 1 day and a gel electrolyte with 10 ml content is formed. Finally, the gel electrolyte formed is then immersed into 1 M of KOH solution and labelled accordingly. Thereafter, the similar preparation procedures are repeated to form gel electrolyte with 15 ml and 20 ml of content in the ratio of 0.5 PVA: 0.34 NCC: 0.167 KOH. Subsequently, the preparation of gel electrolyte is repeated to form gel electrolyte with 20 wt% and 30 wt% of nanocellulose content. Finally, the concentration of the KOH solution substituted with 2 M and 3 M in the similar preparation procedures.

3.5 Preparation of Air Cathode

The preparation method of the air cathode is referred to the method proposed by previous research. The manganese oxide functions as the electrocatalyst while nickel mesh serves as the current collector in the air cathode. The total content required by 1 piece of nickel mesh is 5g. Initially, the carbon black powder , activated carbon powder and manganese oxide is added in a mass ratio of 8:1:1 and mixed using a glass rod, thus forming a powder mixture. Subsequently, 10 ml of Polytetrafluoroethylene (PTFE) and 15 ml of Propanol is added bit by bit into the powder mixture. While adding the PTFE and Propanol, the mixture is stirred continuously using a glass rod. This mixture will slowly form into paste texture. After that, the nickel mesh is coated with the paste formed earlier and subject to rolling using a rolling pin to allow the pasted coated evenly on the nickel mesh and form an air cathode. After that, the air cathode is allowed to dry at ambient temperature.

3.6 Design and Assembly of Battery

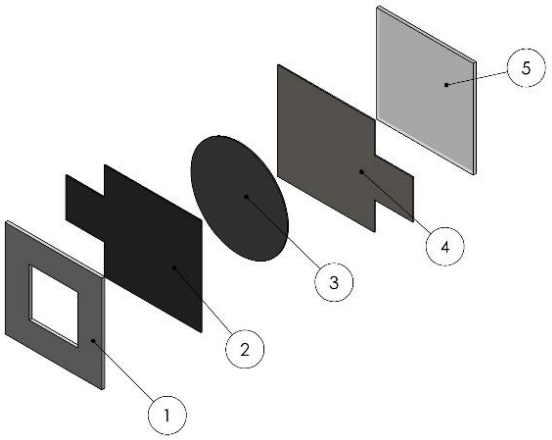

ITEM NO.	PART NUMBER
1	Top Acrylic
2	Air Cathode
3	Gel Electrolyte
4	Al Anode
5	Bottom Acrylic

Figure 3.2: Design of the Al-air Battery.

The components involved in the Al-air battery are the aluminium anode, the air cathode, the gel electrolyte, and the battery case. The design configuration of the AAB is presented as in figure 3.1. The battery case is made of 2 acrylic plates with dimensions of 40 mm × 40 mm and 3 mm for thickness. However, one of the acrylic plates consist of a center cut section with 20 mm × 20 mm to allow the air from the surrounding to pass through and get in contact with the air cathode for the chemical reactions required. The aluminium anode and the air cathode were cut to shape of rectangle with dimensions of 40 mm × 30 mm whereas the gel electrolyte is cut into quarter-circle shape. Generally, the assembly of the Al-air battery follows in an order beginning with a centered extruded top acrylic plate, the air cathode, the gel electrolyte, following with an aluminium anode and finally ending with a bottom acrylic plate. Binders are used to clamp the battery case when assembling the battery to ensure the components in between the acrylic plates are fixed accordingly. Figure 3.2 below depicts the assembly of the fabricated Al-air battery which ready to battery performance testing.

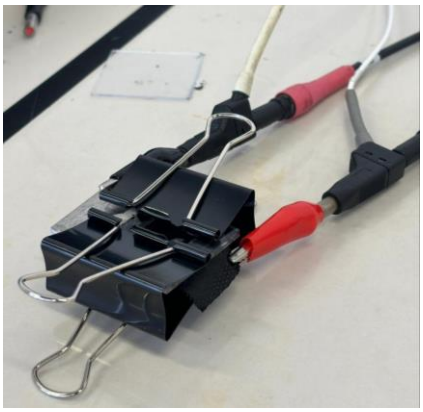

Figure 3.3: Assembly of Al-air Battery.

3.7 Battery Performance Analysis

In essence, the research aims to study the performance of the Al-air battery using a thin film cellulose gel electrolyte and investigate how varying the concentration of KOH, the thickness of the gel electrolyte and the content of nanocellulose impacts the battery's performance. There are few types of analysis involved in this research which includes Constant Current Discharge test, Polarization test, SEM analysis, Corrosion Test, Water Retention Test and Shrinkage Test. With different composition of gel electrolyte, the performance of the Al-air battery could vary including the discharging time of the battery, the open-circuit voltage, the current density, and the rate of the rate of corrosion on the Al anode. These analyses were carried out to review and determine the best performing Al-air battery.

3.7.1 Polarization Test

The investigation of the polarization characteristics of the Al-air battery integrated with thin film cellulose gel electrolyte, the electrocatalytic performance of the Cathode and the anodic potentiodynamic of the Al anode were done using the polarization test. The polarization test was conducted at a scan rate of 5 mA/s and the polarization characteristic of the Al-air battery was presented in a curve graph having potential as the y-axis while current density as the x-axis.

3.7.2 Constant Current Discharge Test

The discharging performance of the Al-air battery was assessed using a constant current discharge test. The Al-air battery integrated with thin film cellulose gel electrolyte was discharged at 10 mA for a certain period. The discharging performance results as a curve graph with cell voltage as y-axis and time as x-axis. After that, the test was conducted again with gel-electrolyte of different thickness, KOH concentrations and NCC contents to evaluate the Al-air battery showing the optimal performance and conclude how varying the concentrations within the thin film cellulose gel electrolyte affect the overall performance of the battery. Subsequently, the test was repeated with discharging current of 50 mA and 100 mA specifically for the thin film cellulose gel electrolyte with 3 M of KOH.

3.7.3 Corrosion Test

The corrosion rate of the aluminium anode is determined by measuring its weight before and after the discharge test. After discharging, the anode is taken out of the assembly and undergoes a 15 minute ultrasonic cleaning to remove surface impurities. An analytical balance is then used to measure the weight of anode, and the corrosion rate is computed using the following equation 3-5.

$$\text{Corrosion Rate } (\text{mg.min}^{-1}.\text{cm}^{-2}) = \frac{\text{W}}{\text{AT}} \quad (3\text{-}5)$$

Where, W is the weight loss for aluminium anode (mg), A is the surface area exposed during discharging (cm^2) and T is the discharge time (min).

3.7.4 Water Absorption Test

The investigation of the water absorption ability of the gel electrolytes fabricated is assessed by measuring the weight of gel electrolyte before and after the discharge test. Upon the completion of discharging test, an analytical balance is used to measure the weight of the gel electrolyte and the water absorption is calculated with the equation 3-6 below.

$$\text{Water Absorption } (\%) = \frac{\text{W}_{\text{before}} - \text{W}_{\text{after}}}{\text{W}_{\text{before}}} \times 100\% \quad (3\text{-}6)$$

Where, W_{before} is the weight of the gel electrolyte before discharging test and W_{after} is the weight of the gel electrolyte after discharging test.

3.7.5 Shrinkage Test

The shrinkage effect of the gel electrolytes is determined by measuring the difference in the dimensions of the gel electrolyte including the surface area, thickness and volume. As the gel electrolyte is fabricated, an analytical balance is used to measure the initial dimensions of the gel electrolyte before undergoing the discharging test. Upon the completion of discharging test, the final dimensions of the gel electrolyte are measured again, and the shrinkage effect is computed using the following equation 3-7.

$$\text{Shrinkage } (\%) = \frac{V_{before} - V_{after}}{V_{before}} \times 100\% \quad (3\text{-}7)$$

Where, V_{before} is the volume of the gel electrolyte before discharging test and V_{after} is the volume of the gel electrolyte after discharging test.

3.7.6 Reusability Test

The ability of the thin film cellulose gel electrolyte to perform consistently over multiple discharge cycles is determined using the reusability test. The thin film cellulose gel electrolyte used for the reusability test is made with a composition of 10 wt% PVA, 10 wt% NCC, and 1 M KOH, maintaining a 20 ml content volume. The reusability test is conducted in which the thin film cellulose gel electrolyte is subjected to several sets of polarization and discharge test. After each test cycle, the thin film cellulose gel electrolyte is soaked in KOH solution for one day before proceeding with the next set of tests.

3.7.7 SEM Analysis & EDAX

The surface morphologies of the gel electrolytes fabricated are analyzed using the Scaninng Electron Microscopy (SEM). The SEM images for the morphologies of the gel electrolyte is captured using magnification of 500x. The Energy Dispersive X-ray Analysis (EDAX) is used to determine the elemental

composition of the powder formed from the discharging test and an elemental mapping is generated revealing the he distribution of specific elements across the surface of the powder formed.

3.8 Gantt Chart

This section presents the Gantt chart scheduled for final year project part 1 and part 2 which includes the timeline for report writing, journal researching, method researching, material procurement, material preparation, battery fabrication and battery testing. The schedule covers from week 1 until week 14 of final year project part 1 and part 2.

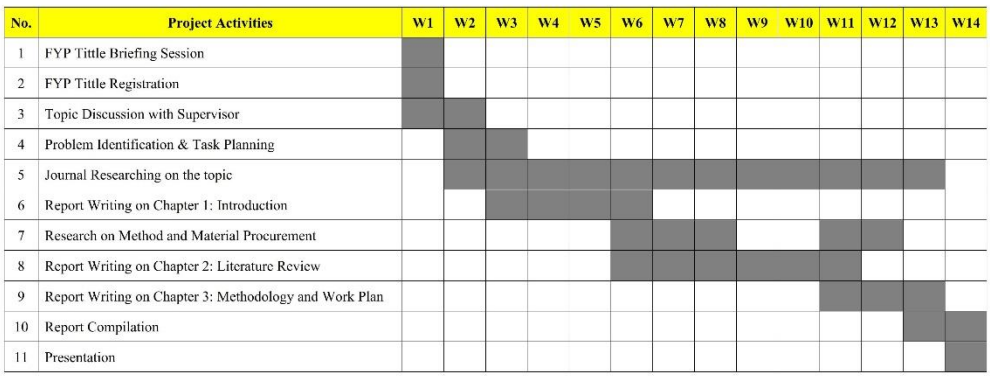

No.	Project Activities	W1	W2	W3	W4	W5	W6	W7	W8	W9	W10	W11	W12	W13	W14
1	FYP Tittle Briefing Session														
2	FYP Tittle Registration														
3	Topic Discussion with Supervisor														
4	Problem Identification & Task Planning														
5	Journal Researching on the topic														
6	Report Writing on Chapter 1: Introduction														
7	Research on Method and Material Procurement														
8	Report Writing on Chapter 2: Literature Review														
9	Report Writing on Chapter 3: Methodology and Work Plan														
10	Report Compilation														
11	Presentation														

Figure 3.4: Gantt Chart for Final Year Project Part 1.

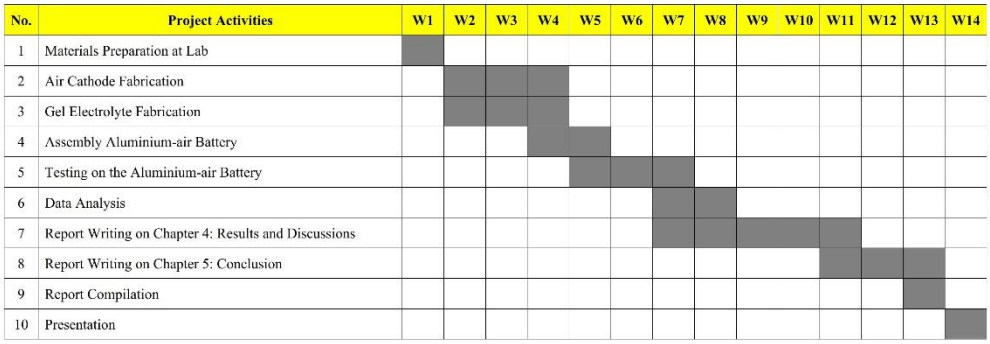

No.	Project Activities	W1	W2	W3	W4	W5	W6	W7	W8	W9	W10	W11	W12	W13	W14
1	Materials Preparation at Lab														
2	Air Cathode Fabrication														
3	Gel Electrolyte Fabrication														
4	Assembly Aluminium-air Battery														
5	Testing on the Aluminium-air Battery														
6	Data Analysis														
7	Report Writing on Chapter 4: Results and Discussions														
8	Report Writing on Chapter 5: Conclusion														
9	Report Compilation														
10	Presentation														

Figure 3.5: Gantt Chart for Final Year Project Part 2.

CHAPTER 4

RESULTS AND DISCUSSIONS

4.1 Effect of Gel Electrolyte Thickness

With the current implementation of Al-air battery technology, the performance of the battery is often associated with factors involving thickness of the gel electrolyte, nanocellulose content incorporated into the gel electrolyte and the concentration of alkaline electrolyte. The gel electrolyte is crucial as it serves as reservoir to retain a significant amount of alkaline based electrolyte and act as a medium to ensure consistent ion transfer during an electrochemical reaction as well as to isolate the Aluminium anode and Air cathode to prevent short circuit of the battery. While a thinner gel electrolyte can reduce the ionic resistance during the discharging of the battery, it may affect the peak power density and discharging period of the battery by retaining lesser amount of electrolyte and increases the risk of short circuits due to the interaction between the Aluminium anode and Air cathode. Therefore, the gel electrolyte thickness must be optimized to allow a consistent and superior performance of the Al-air battery. However, fabricating a gel electrolyte with a precise thickness presents several challenges. It requires meticulous control over the amount of material added, and the thickness can be easily influenced by factors such as solvent evaporation during the thawing process. Achieving and maintaining a specific thickness demands high precision in measurement and careful management of environmental factors. Nonetheless, controlling the gel electrolyte thickness in terms of volume of the content added into the gel electrolyte is much easier especially in laboratory settings. Essentially, the volume of the content added into gel electrolyte is directly related to the thickness of the gel electrolyte. In this study, 3 different thickness of gel electrolyte were fabricated which consist of 10 ml , 15 ml and 20 ml of content in the gel electrolyte. The contents consist of 10 wt% of nanocellulose, 10 wt% of Polyvinyl Alcohol (PVA) and 1 M of Potassium Hydroxide solution and kept in the same ratio for all 3 different thicknesses. According to Table 3.1, the thickness of the gel electrolyte fabricated based on the respective volume of content added are 0.71 mm for 10 ml, 0.8 mm for 15 ml and 1.26 mm for 20 ml. Polarization test and constant

current discharge test were performed to compare the effect of gel electrolyte with different thickness on the performance of the Al-air battery.

According to the polarization test results as depicted in Figure 4.1, it reveals that the gel electrolyte with 0.8 mm and 1.26 mm thickness achieve higher peak power density of 98 mW and 90 mW as compared to 72 mW from gel electrolyte with 0.71 mm thickness. While the thicker gel electrolyte may result in higher ionic resistance within the battery due to longer ion travel distance, but the increased retention of alkaline electrolyte compensates the resistance, maintaining a stable voltage and thus improving the peak power density of the Al-air battery. However, the gel electrolyte with 0.8 mm has a higher open circuit voltage (OCV) of 1.98 V as compared to 1.85 V and 1.86 V from gel electrolyte with 0.71 mm and 1.26 mm thickness. Nonetheless, no noticeable differences in voltage drop are observed at low current densities, also known as the activation region. In this region, the voltage drop is primarily due to the kinetics of the electrochemical reactions at the catalytic surface. Therefore, when comparing Al-air batteries with three different gel electrolyte thicknesses, the voltage drop remains similar because the same air cathode is used in the experiments. As the current density increases, the voltage begin to drop linearly due to the ohmic resistance within the battery. However, the gel electrolyte with thickness of 0.71 mm show more voltage drop than the gel electrolyte with thickness of 0.8 mm and 1.26 mm. This suggested that the greater retention of alkaline electrolyte in thicker gel electrolyte helps to compensate the higher ohmic resistance within the battery contributing to higher voltage output. At high current densities, the voltage drop mainly due to mass transport. It is revealed that the gel electrolyte with 1.26 mm of thickness can achieve a discharge current of 127 mA whereas gel electrolytes with 0.71 mm and 0.8 mm of thickness can only achieve 87 mA and 108 mA. This indicates that a 1.26 mm thick gel electrolyte is optimal, providing sufficient alkaline electrolyte retention without excessively hindering ion movement and electrochemical reaction rates. According to the comparison of discharge curve for Al-air battery with gel electrolyte of different thickness as shown in Figure 4.2, it indicates that the discharging performance of Al-air battery with 1.26 mm of gel electrolyte outperform both the batteries with 0.71 mm and 0.8 mm of gel electrolyte. The discharge current used in the discharge test is 10 mA. The Al-

air battery with 1.26 mm of gel electrolyte thickness can discharge for 95 minutes while the other 2 gel electrolyte can only discharge for 75 and 84 minutes respectively.

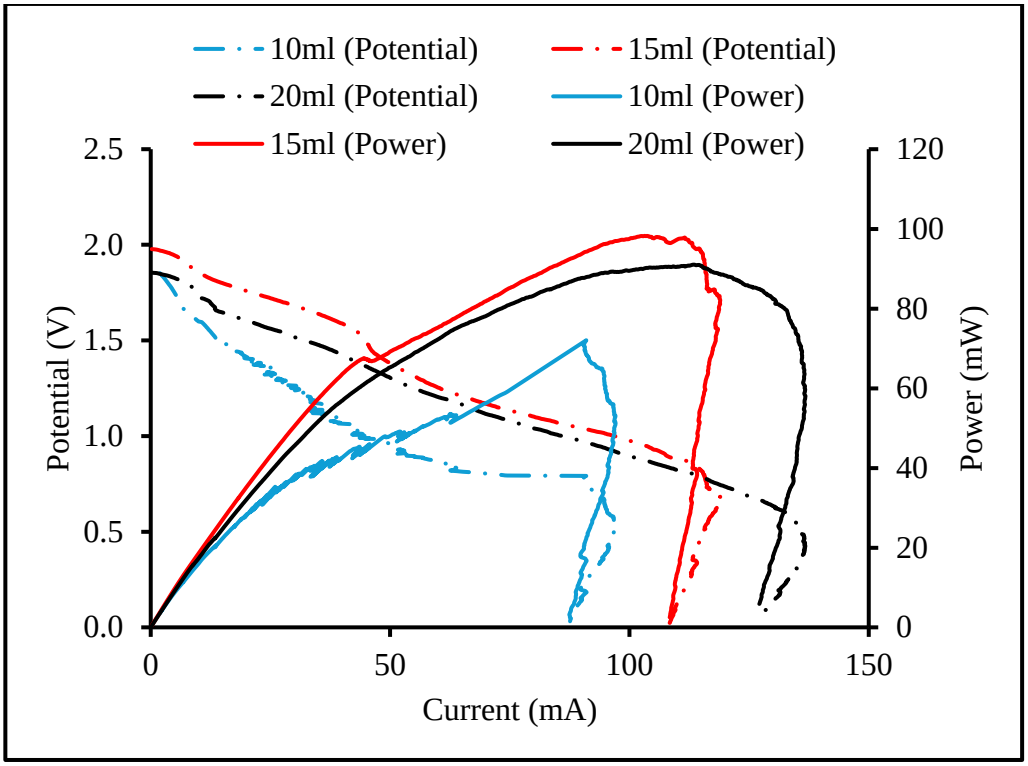

Figure 4.1: Polarization Curve for Al-air Battery with Gel Electrolyte of Different Thickness.

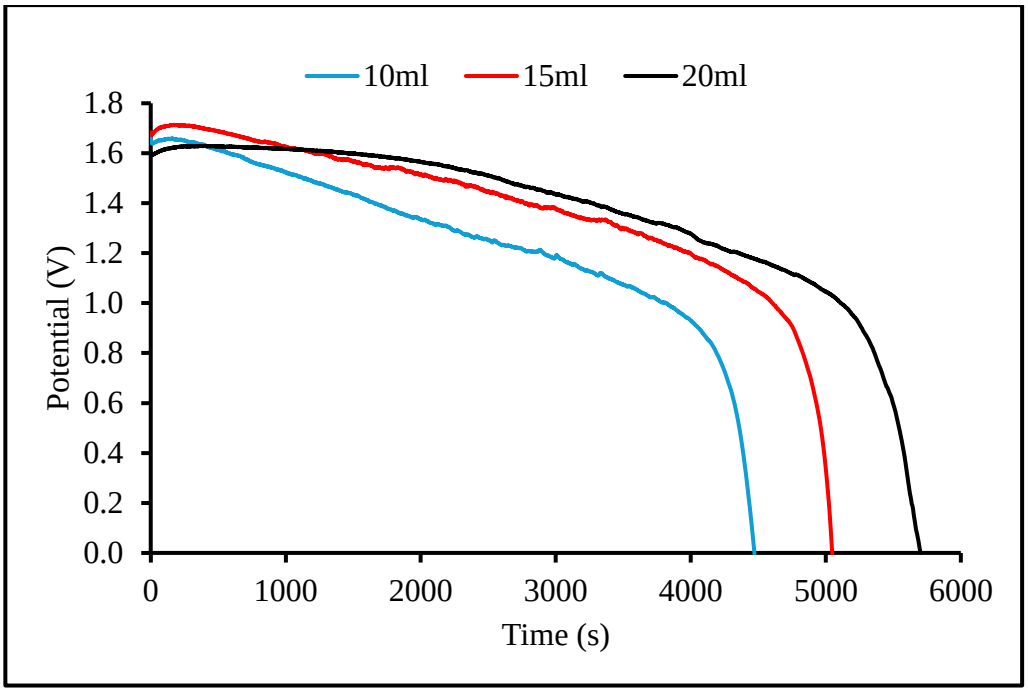

Figure 4.2: Discharge Curve for Al-Air Battery with Gel Electrolyte of Different Thickness.

Other than that, the tendency to undergo self-corrosion at the Aluminium anode remains as a major hindrance of the Al-air battery as it is unavoidable. Hence, corrosion test is conducted to discover the effect of gel electrolyte with different thickness on the corrosion rate of the Aluminium anode. The test was conducted by attaching the gel electrolyte of different thickness onto the Aluminium anode for 4 hours and computations of corrosion rate involving the area contact between the Aluminium anode and gel electrolyte, time of discharging and difference in mass of Aluminium anode are made. According to Figure 4.3, it reveals that the corrosion rate of gel electrolyte with 1.26 mm thickness is the highest at 0.08456 $mg.min^{-1}.cm^{-2}$ compared to 0.01712 $mg.min^{-1}.cm^{-2}$ and 0.02957 $mg.min^{-1}.cm^{-2}$. The corrosion of Aluminium anode is more favourable with the presence of more electrolyte which depends on the electrolyte retention of the gel electrolyte. Hence, gel electrolyte with 1.26 mm thickness with the better electrolyte retention implies the highest corrosion rate of Aluminium anode. Furthermore, water absorption test is conducted to identify whether thicker gel electrolyte has higher electrolyte retention ability. The water absorption test is conducted by measuring the difference in mass of the gel electrolytes before and after discharging. It reveals in Figure 4.4 that

water absorption of gel electrolyte with 1.26 mm thickness is higher at 18.45% as compared to 17.80% and 18.02% for 0.71 mm and 0.8 mm. Despite that higher electrolyte retention contributes to higher corrosion rate of Aluminium anode, it is the primary factor that enhances the electrochemical and discharge performance of the Aluminium-air battery. Aside from that, shrinkage of gel electrolyte can potentially lead to poor contact between the gel electrolyte, the aluminium anode and the air cathode which affects the battery performance and eventually short-circuit the battery. Hence, Shrinkage test is conducted to identify the shrinkage effect on different gel electrolyte thickness. According to Figure 4.5, it reveals that the gel electrolyte with 0.71 mm thickness has the highest shrinkage effect of 60.76% following by 56.78% from 0.8 mm thickness and 44.42% from 1.26 mm thickness. The shrinkage effect are generally due to poor electrolyte retention as the electrolyte evaporates when exposed to ambient conditions leading to reduction in the gel electrolyte volume. Therefore, with the lower electrolyte retention from gel electrolyte with 10 ml thickness results in the higher shrinkage effect of the gel electrolyte.

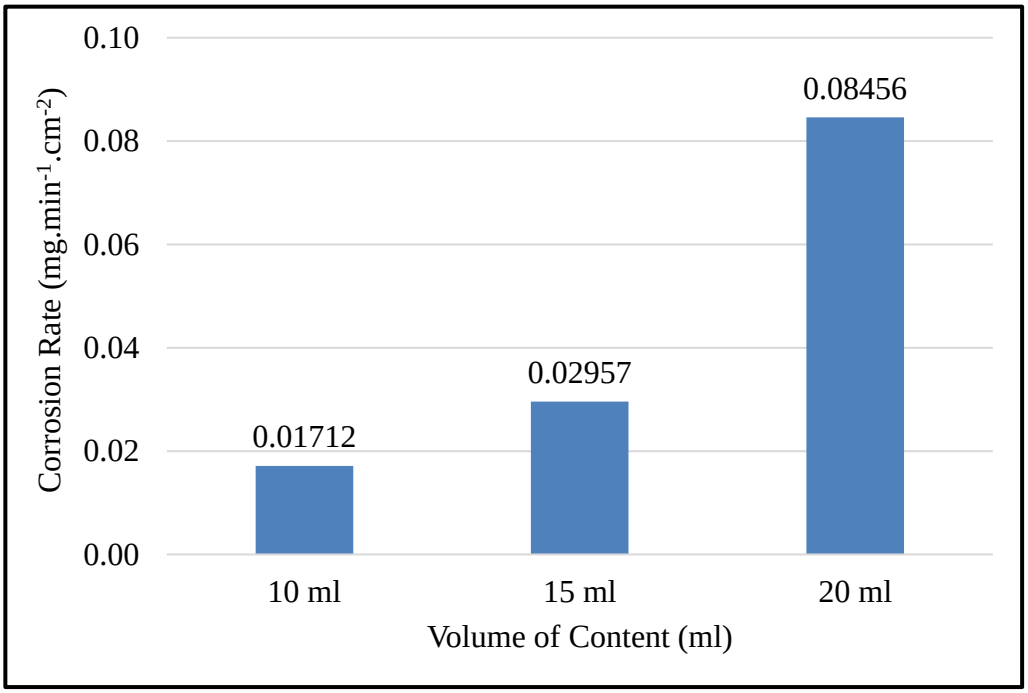

Figure 4.3: Corrosion Rates for Al-Air Battery with Gel Electrolyte of Different Thickness.

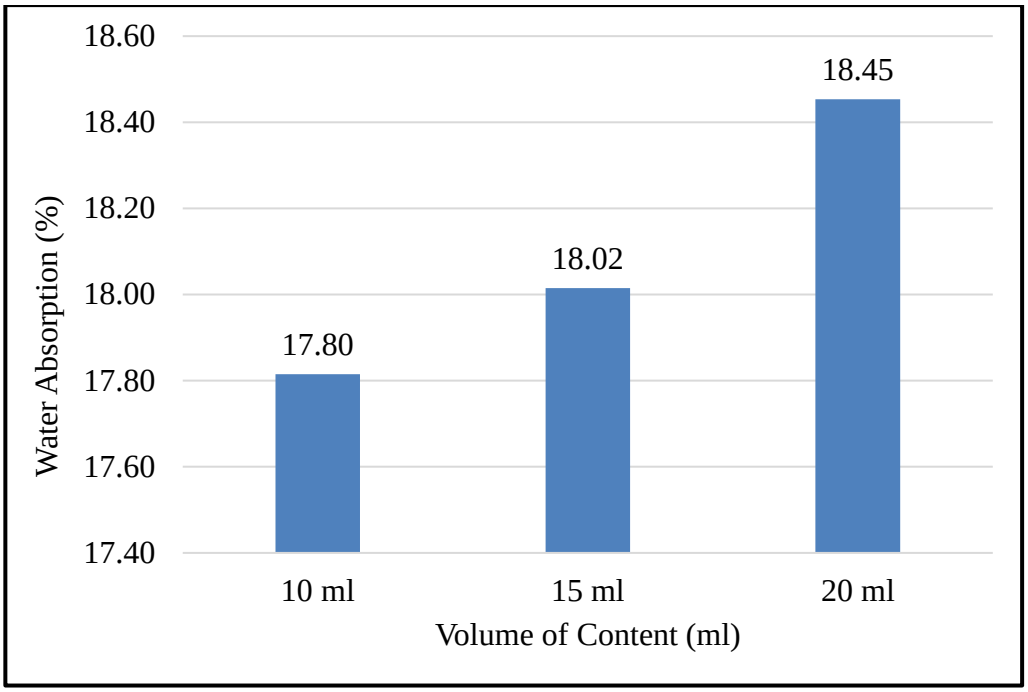

Figure 4.4: Water Absorption for Al-Air Battery with Gel Electrolyte of Different Thickness.

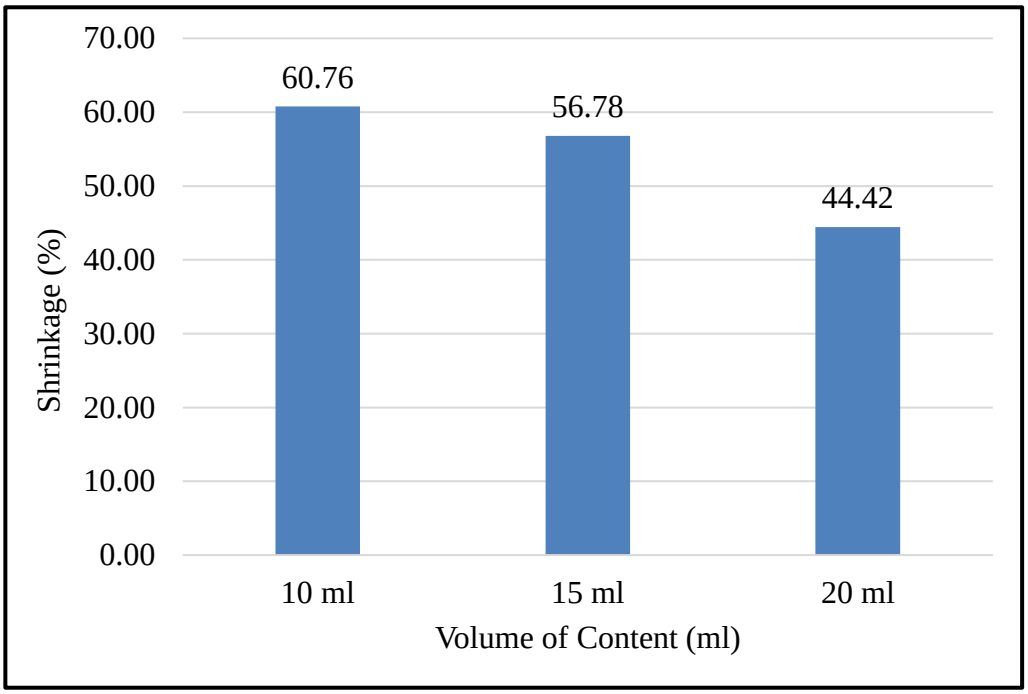

Figure 4.5: Shrinkage for Al-Air Battery with Gel Electrolyte of Different Thickness.

Table 4.1: Summary of Properties for Gel Electrolyte with Different Thickness.

Volume of Content	10 ml	15 ml	20 ml
Thickness (mm)	0.71	0.8	1.26
Open Circuit Voltage (V)	1.85	1.98	1.86
Peak Power Density (mW)	72	98	91
Discharge Time (minutes)	75	84	95
Corrosion Rate ($mg.min^{-1}.cm^{-2}$)	0.01712	0.02957	0.08456
Water Absorption (%)	17.80	18.02	18.45
Shrinkage (%)	60.76	56.78	44.42

On top of that, SEM was conducted to characterize the surface morphology of the gel electrolyte with different thicknesses. Since the composition of these gel electrolytes with different thicknesses are similar, it reveals that all the gel electrolytes surface appears to be uneven with dense and rugged texture. Due to the incorporation of nanocellulose, there are noticeable crosslinked structure forming interconnected voids within the gel electrolyte. These voids indicates the porosity in the gel electrolyte which are the reason why gel electrolytes can act as an electrolyte reservoir and retain electrolyte. Although all the gel electrolyte exhibits particles with pores, but the density of pores have distinguishable differences. The surface of gel electrolyte with 1.26 mm thickness show relatively denser pores as compared to the compact surface of gel electrolyte with 0.71 mm and 0.8 mm thicknesses. The denser porous structure of gel electrolyte with 1.26 mm thickness is more conducive to improving absorption and retention of alkaline electrolyte which facilitates the ion transfer during the electrochemical process. Overall, the gel electrolyte with a thickness of 1.26mm which fabricated using 20 ml of content added into the gel electrolyte delivers the best performance for the Al-air battery. Therefore, subsequent experiments and tests will be carried out using the similar volume of content.

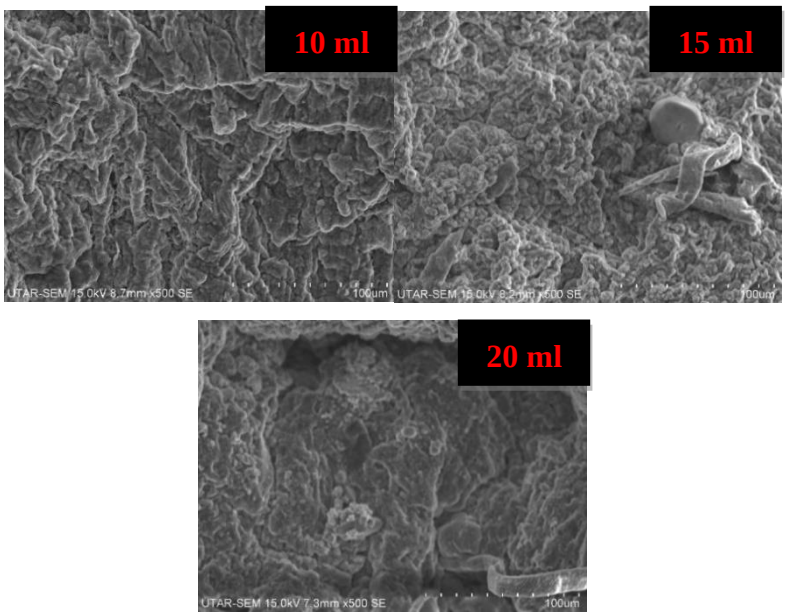

Figure 4.6: SEM Image of 500x magnification of Thin Film Cellulose Gel Electrolyte with 0.71 mm, 0.8 mm and 1.26 mm of Thickness.

4.2 Effect of Nanocellulose (NCC) Content

While the gel electrolyte is able to eliminate problems such as leakage of electrolyte and act as a separator for Al-air battery to prevent short-circuit, it often come with a drawback of having low ionic conductivity with short discharging period. These issues are often related to the electrolyte uptake ability of the gel electrolyte as more alkaline electrolyte are retained in the gel electrolyte and the transference of ions is more favorable during an electrochemical reaction. There is limited amount of research focused on the incorporation of nanocellulose into the gel electrolyte especially for the usage of Al-air battery. While incorporating nanocellulose into the gel electrolyte can enhance the structural properties and increases the porosity of a gel electrolyte, excessive amount may affect the ionic conductivity of the gel electrolyte and negatively impact on the performance of the Al-air battery. Therefore, the nanocellulose content added into the gel electrolyte is needed to be optimized. Several thin film cellulose gel electrolytes were fabricated by incorporating 10 wt%, 20 wt% and 30 wt% of nanocellulose (NCC) content. Furthermore, a gel electrolyte fabricated with only 10 wt% of PVA and 1 M of KOH is used as a benchmark and compare with the thin film cellulose gel electrolyte. Polarization test and constant current discharge test were performed to compare the effect of

gel electrolyte with and without nanocellulose as well as the impact of NCC content on the performance of the Al-air battery.

Based on the polarization test as shown in Figure 4.7, the Al-air battery incorporated with thin film cellulose gel electrolyte of 10 wt% NCC content achieve higher peak power density of 91 mW as compared to 55 mW from the gel electrolyte without NCC content. It also reveals that the open circuit voltage (OCV) of the gel electrolyte without nanocellulose presents higher at 2.01 V as compared to 1.86 V for the thin film cellulose gel electrolyte. The incorporation of nanocellulose enhances the ionic conductivity of the gel electrolyte by creating more porous structures within the gel electrolyte which allow greater electrolyte retention ensuring the consistent ion movement during the electrochemical reaction. Despite the benefits of incorporating nanocellulose into gel electrolytes, increasing the NCC content to 20 wt% and 30 wt% can lead to a reduction in peak power density, with values dropping to 82 mW and 75 mW, respectively, compared to the 10 wt% NCC content. However, the OCV of the gel electrolyte with 10 wt% NCC content is lower at 1.86 V compared to 1.93 V and 2.01 V for the gel electrolyte with 20 wt% and 30 wt% NCC content. The excessive nanocellulose content added into the gel electrolyte create a denser and more compact gel structure which increases the internal resistance and hinders the ion movement. Furthermore, the excessive nanocellulose may fill the pores within the gel electrolyte and limit the electrolyte retention of the gel electrolyte resulting the lower peak power density. According to the comparison of polarization curve for different NCC content, it reveals that the voltage drop at the low current densities are insignificant for all the gel electrolytes as the same air cathode is used in the experiment, thus having the same catalytic surface for electrochemical reactions. However, when the current density increases, the voltage begin to drop linearly due to the ohmic resistance within the battery. It reveals that the gel electrolyte without nanocellulose consists of a steeper voltage drop as compared to the thin film cellulose gel electrolyte of 10 wt% NCC content. This suggested that the dense and compact structure within the gel electrolyte without nanocellulose has a higher ohmic resistance as compared to the porous structure formed in the thin film cellulose gel electrolyte. Aside from that, when comparing the gel electrolyte of 10 wt% NCC to those with 20 wt% and 30 wt%, it reveals that the voltage drop for the

higher NCC content is steeper. The excessive nanocellulose filling the pores within the gel electrolyte increases the overall ohmic resistance and limiting the ionic pathway, therefore resulting the more significant voltage drop. At high current densities, the voltage loss is primarily due to mass transport. The gel electrolyte without nanocellulose can only achieve a discharge current of 47 mA whereas the thin film cellulose gel electrolyte with 10 wt%, 20 wt% and 30 wt% can achieve 127 mA, 102 mA and 82 mA respectively. This indicates that electrochemical performance of the Al-air battery incorporated with thin film cellulose gel electrolyte is higher than those with gel electrolyte without nanocellulose and highlight the negative impact of excessive nanocellulose in gel electrolyte, therefore, suggesting that 10 wt% NCC content is preferred.

According to the discharge curves as shown in Figure 4.8, the discharging period for the Al-air battery incorporated with thin film cellulose gel electrolyte of 10 wt% NCC content is significantly longer at 95 minutes compared to 43 minutes for the gel electrolyte without nanocellulose. The electrolyte uptake ability is crucial for better discharging performance. The results signifies the better electrolyte retention of the thin film cellulose gel electrolyte which have a more porous structure which results in a longer discharging period. The discharging period of thin film cellulose gel electrolyte of 10 wt% NCC content remains the longest when compared to those with 20 wt% and 30 wt% NCC content at 78 minutes and 60 minutes respectively. While the higher NCC content can create porous structure within the gel electrolyte, but it also create a dense and compact network at the same time. The ion movements is significantly hindered by the dense structure and the electrolyte retention is weaken due to the voids filled by the nanocellulose.

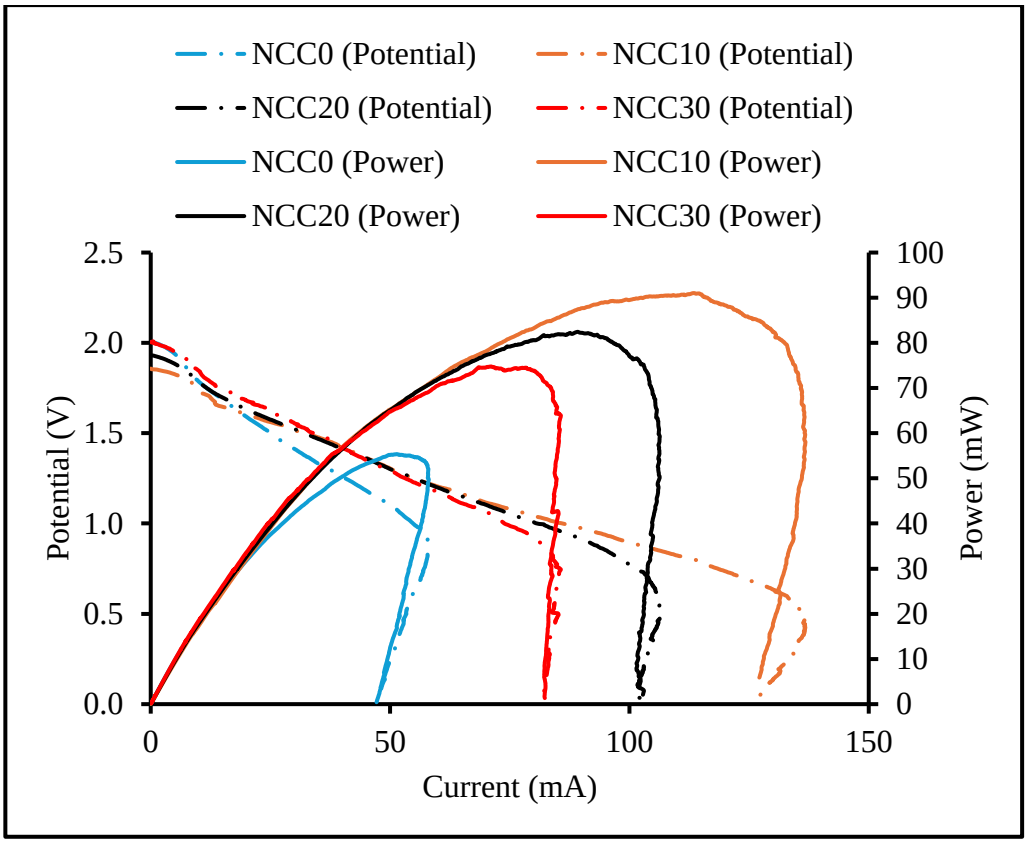

Figure 4.7: Polarization Curve for Al-air Battery with Gel Electrolyte of Different NCC Content.

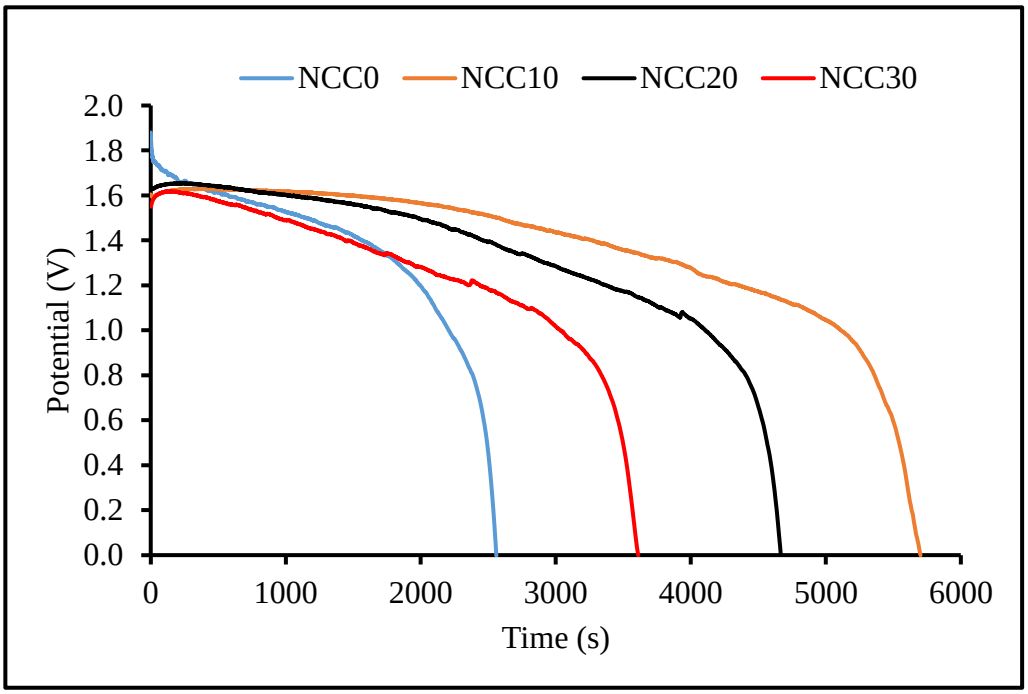

Figure 4.8: Discharge Curve for Al-Air Battery with Gel Electrolyte of Different NCC Content.

Besides that, corrosion test is performed to investigate the corrosion rate of the Aluminium anode with the gel electrolyte without nanocellulose as well as the gel electrolyte with different NCC content. With 4 hours of corrosion testing, it reveals in Figure 4.9 that the corrosion rate of the gel electrolyte without nanocellulose is lower at 0.00514 $mg.min^{-1}.cm^{-2}$ compared to 0.08456 $mg.min^{-1}.cm^{-2}$ for the gel electrolyte with 10 wt% NCC content. Furthermore, the gel electrolyte with 20 wt% and 30 wt% NCC content also reveals a lower corrosion rate than 10 wt% NCC content at 0.03214 $mg.min^{-1}.cm^{-2}$ and 0.00511 $mg.min^{-1}.cm^{-2}$ respectively. This generally implies the corrosion of Aluminium anode tends to be unavoidable for the gel electrolyte with higher electrolyte retention which allow superior electrochemical reaction. Furthermore, the water absorption test is conducted to rectify the electrolyte retention of the gel electrolytes. According to the Figure 4.10, the water absorption ability of the thin film cellulose gel electrolyte with 10 wt% NCC content is 18.45% which suggest an improvement of 35% better than the gel electrolyte without nanocellulose at 13.66%. The improvement in water absorption ability of the thin film cellulose gel electrolyte is primarily contributed from the porosities created by the crosslinking featured from the nanocellulose incorporated. Additionally, the results from the water absorption test also suggested that thin film cellulose gel electrolyte with 20 wt% and 30 wt% NCC content has lower electrolyte retention of 12.92% and 12.30% as compared to 10 wt% NCC content. This is due to the filling of excessive nanocellulose in the porosities limits the vacancy of pores within the gel electrolyte and reduces the electrolyte uptake ability. As mentioned above, the shrinkage effect can lead to short-circuit which is undesirable as the contact between the Aluminium anode, gel electrolyte and air cathode reduces. According to the results shown in Figure 4.11, the gel electrolyte incorporated with 10 wt% NCC content has a lesser shrinkage effect of 44.42% as compared to gel electrolyte without nanocellulose which have 60.02% of shrinkage effect. The significant shrinkage of the gel electrolyte without nanocellulose is closely related to its poor electrolyte retention. As with lower water absorption ability, the gel electrolyte retains lesser electrolyte, making it more prone to evaporation under ambient conditions and rapid consumption during discharge causing the gel electrolyte to shrink. The shrinkage effect in the thin film cellulose gel electrolyte with 20

wt% and 30 wt% NCC content is significantly higher, at 59.71% and 50.80% respectively, compared to the 10 wt% NCC content. This increased shrinkage is due to the clumping of particles, as the excessive nanocellulose fills the pores, leading to structural instability. Additionally, the denser gel structure resulting from the higher NCC content reduces the available volume for electrolyte capacity. As a result, electrolyte is consumed more rapidly, and the shrinkage effect increases.

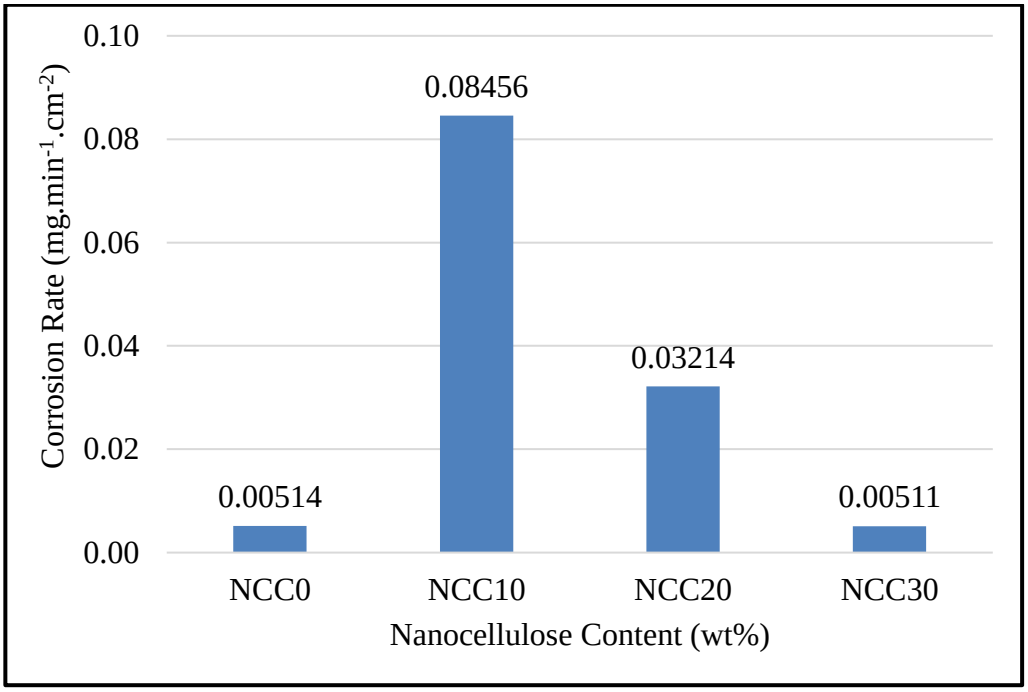

Figure 4.9: Corrosion Rate for Al-air Battery with Gel Electrolyte of Different NCC Content.

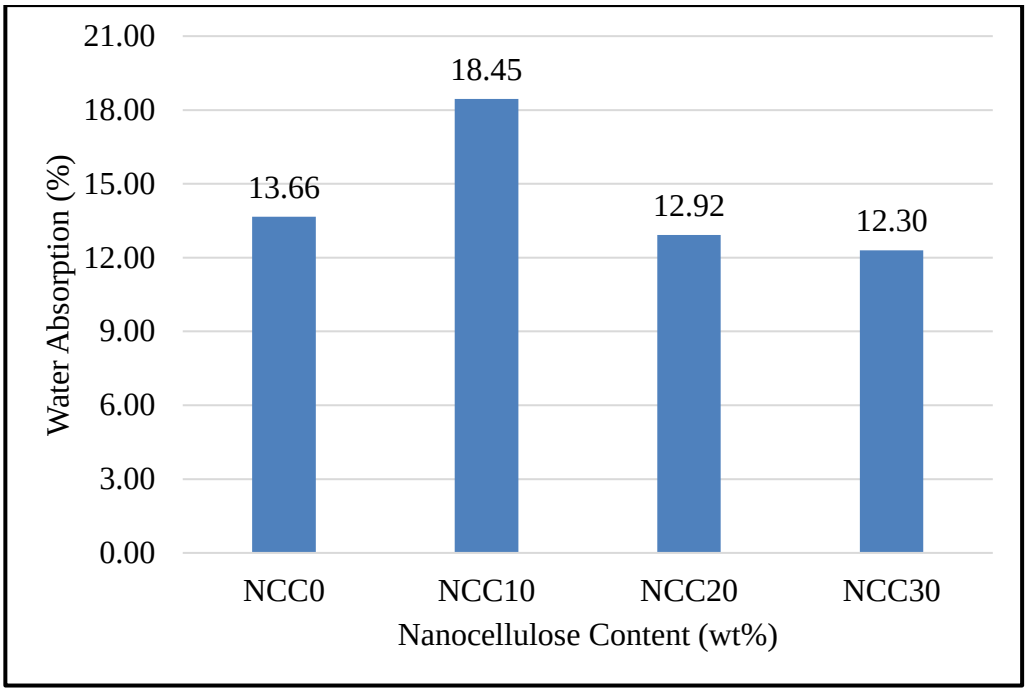

Figure 4.10: Water Absorption for Al-air Battery with Gel Electrolyte of Different NCC Content.

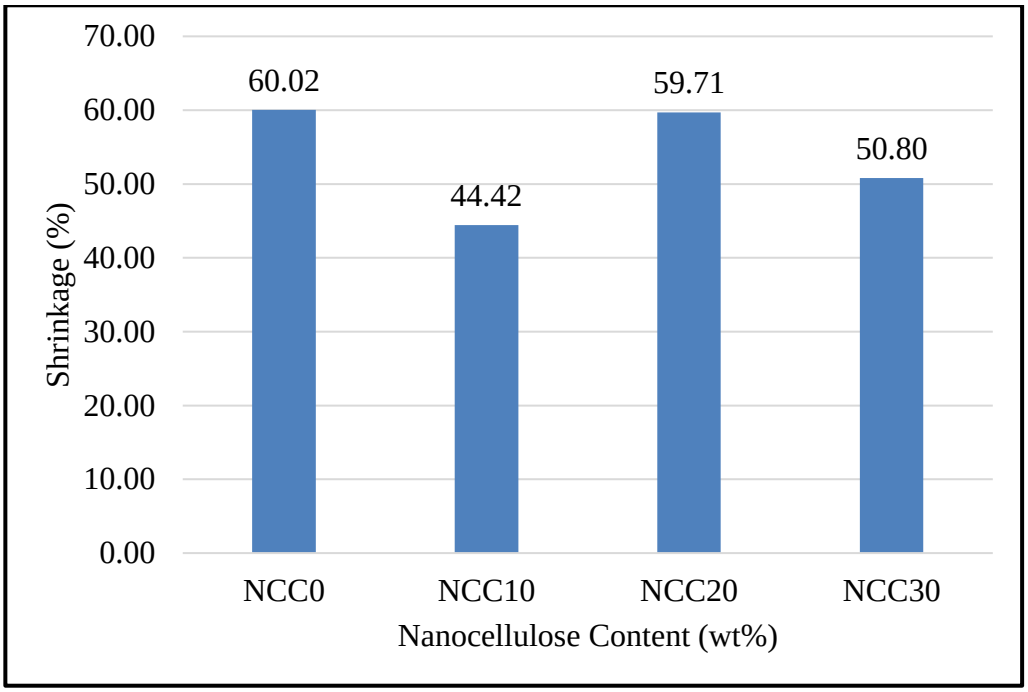

Figure 4.11: Shrinkage for Al-air Battery with Gel Electrolyte of Different NCC Content.

Table 4.2: Summary of Properties for Gel Electrolyte with Different NCC Content.

NCC Content	0 wt%	10 wt%	20 wt%	30 wt%
Open Circuit Voltage (V)	2.01	1.86	1.93	2.01
Peak Power Density (mW)	55	91	82	74
Discharge Time (minutes)	43	95	78	60
Corrosion Rate ($mg.min^{-1}.cm^{-2}$)	0.00514	0.08456	0.03214	0.00511
Water Absorption (%)	13.66	18.45	12.92	12.30
Shrinkage (%)	60.02	44.42	59.71	50.80

Similarly, SEM was conducted to examine the surface morphology of the gel electrolyte without nanocellulose and the thin film cellulose gel electrolyte with 10 wt%, 20 wt% and 30 wt% NCC content. According to the SEM image as depicted in Figure 4.12, it reveals that surface morphology of the gel electrolyte without nanocellulose consist of rough surface texture with various peaks and ridges which indicates the surface irregularities. Despite there are few void spaces but it indicates limited pores within the gel structure. Alongside the pores, the SEM image also suggest a compact structure as there are several dense regions. This morphology contributes to the weaker water absorption ability and suboptimal electrochemical and discharging performance of the gel electrolyte without nanocellulose. In contrast, the SEM image for the gel electrolyte with 10 wt%, 20 wt% and 30 wt% NCC content also reveals the surface to be uneven with rough surface texture. However, there are noticeable crosslinked structure forming interconnected voids within the thin film cellulose gel electrolytes. Essentially, these voids are the porosity within the gel electrolyte. Nonetheless, the gel electrolyte with 10 wt% NCC content presents more prominent darken region indicating the larger pores size and more porous structure which can accommodate more electrolyte and enhance the electrochemical and discharging performance. On the other hand, both the gel electrolyte with 20 wt% and 30 wt% NCC content presents several elongated ridges which suggest the compact and dense crystalline structure formed by the excessive nanocellulose. There are few regions indicating lighter and darker spots which suggest the darker region as the pores formed by the nanocellulose whereas the lighter spots as the excessive nanocellulose. Despite the presence of pores but the excessive nanocellulose has limited the overall performance of the gel electrolyte. In general, the thin film cellulose gel electrolyte with 10 wt%

NCC content delivers the best performance for the Al-air battery. Hence, making 10 wt% NCC content the most suitable for subsequent experiments and tests.

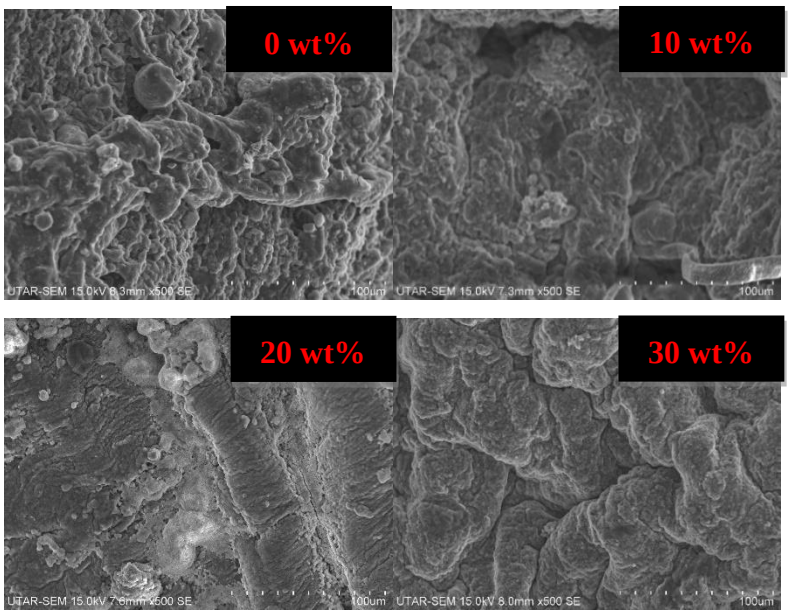

Figure 4.12: SEM Image of 500x magnification of Thin Film Cellulose Gel Electrolyte with 0 wt%, 10 wt%, 20 wt% and 30 wt% of NCC Content.

4.3 Effect of Concentration of Potassium Hydroxide

The concentration of the alkaline electrolyte used in the Al-air battery is one of the important parameters which can affect the performance of the battery. In general, the performance of Al-air battery directly related to the concentration of the alkaline electrolyte as higher concentration of electrolyte indicates more ion transport resulting in faster and better electrochemical performance. In this study, several gel electrolytes are fabricated by varying the concentration of Potassium Hydroxide (KOH) and the total volume of the gel electrolytes are maintain at 20 ml along with the incorporation of 10 wt% NCC content as they showed the best performance during the study on the effect of gel electrolyte thickness and NCC content . Polarization test and constant current discharge test were conducted to compare the effect of gel electrolyte with different concentrations of potassium hydroxide on the performance of the Al-air battery. According to the polarization test results as shown in Figure 4.13, it reveals that

the gel electrolyte with 1 M of KOH achieved the lowest peak power density at 91 mW as compared to 100 mW and 187 mW for 2 M and 3 M KOH respectively. While the volume to for electrolyte capacity are similar as all the gel electrolytes remained with 20 ml volume of content but the increase in concentration of KOH in the gel electrolyte generally enhances the ionic conductivity of the gel electrolyte as there are more hydroxide (OH^-) ions which allows more power output. The gel electrolytes with varying concentrations of KOH have a relatively close value for the open circuit voltage (OCV) of 1.86 V, 2 V and 1.95 V. At low current densities, the voltage drops for all 3 of the gel electrolytes with different concentration of KOH have no tangible differences. This is due to the kinetic limitations of the electrochemical reactions at the air cathode used are same. The increase in current density results in a more significant voltage drop in the ohmic region for the gel electrolyte with 1 M KOH as compared the 2 M and 3 M KOH as there are limited OH^- ions supply in the gel electrolyte. While at high current density, the voltage drop is generally due to mass transport, but it reserves the trend whereby the gel electrolyte with higher concentration, 3 M of KOH achieve a higher discharge current of 232 mA whereas the lower concentrations, 1 M and 2 M of KOH can only achieve 127 mA and 158 mA. Furthermore, from the discharge curve plotted in Figure 4.14, it reveals that the discharging performance are positively correlated with the concentrations of KOH in the gel electrolyte. With a discharging current of 10 mA, the gel electrolyte with 1 M KOH shows a rapid discharging period of 95 minutes from 1.6 V to 0 V. As the concentration of KOH in the gel electrolyte increases to 2 M, the discharging period of the Al-air battery increases to 192 minutes. Nonetheless, with the increment for the concentration of KOH to 3 M, the Al-air battery was able to maintain for 435 minutes which is approximately 7 hours before the energy is depleted. With a higher concentration of KOH in the gel electrolyte, the supply of OH^- ions are surplus facilitating a more consistent ion transport which enhances the ionic conductivity making it more favorable for the superior electrochemical performance of the Al-air battery. With the outstanding discharging performance of gel electrolyte with 3 M KOH, discharge test is conducted with varying current to discover the performance. According to Figure 4.15, it reveals that discharging the Al-air battery with higher current results in a lower

discharging period. As a result, the gel electrolyte was only able to maintain for about 98 minutes with discharging current of 50 mA whereas with the current of 100 mA, the discharging time diminishes to 30 minutes only. This is due to the quicker consumption of OH^- ions as higher current is applied.

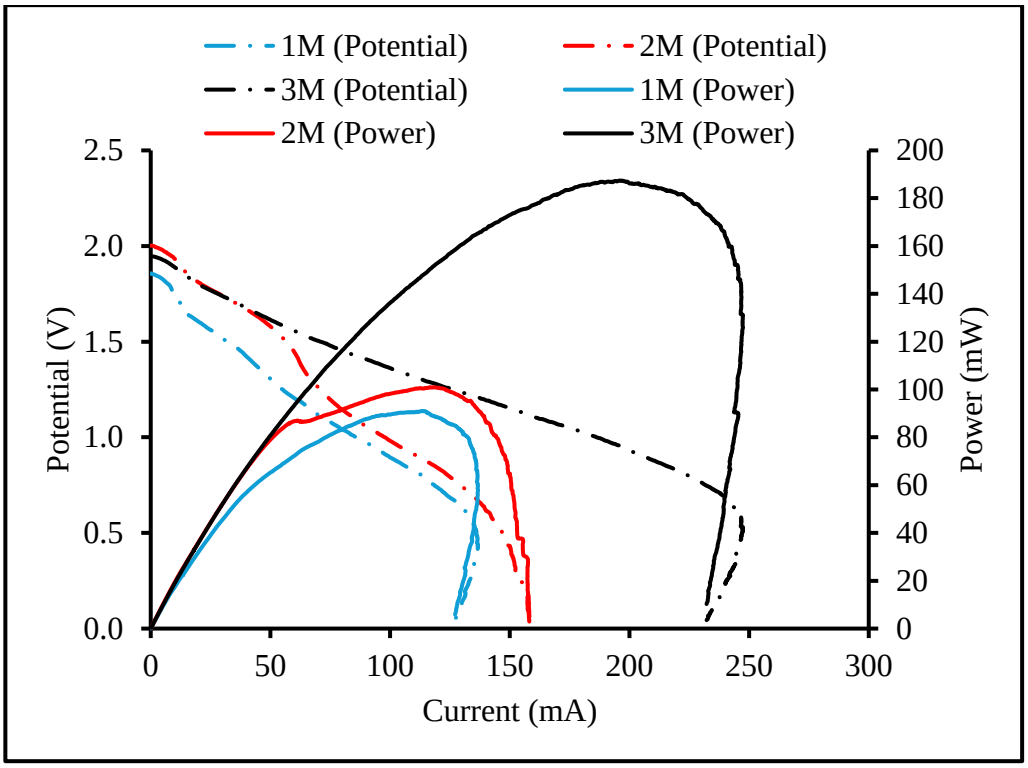

Figure 4.13: Polarization Curve for Al-air Battery with Gel Electrolyte of Different Concentration of Potassium Hydroxide.

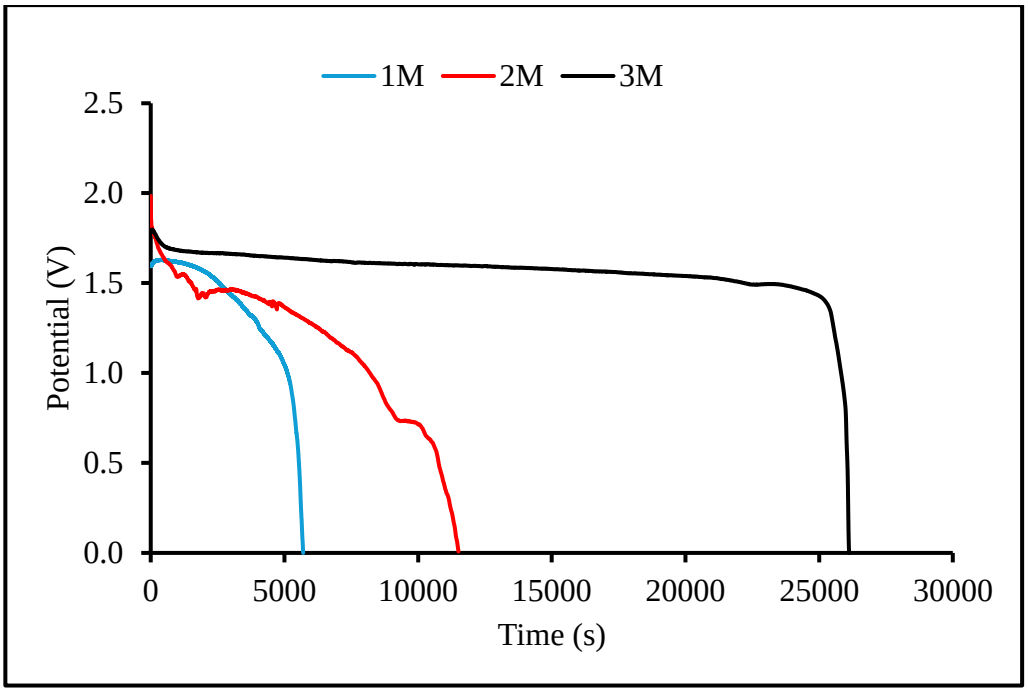

Figure 4.14: Discharge Curve for Al-Air Battery with Gel Electrolyte of Different Concentration of Potassium Hydroxide.

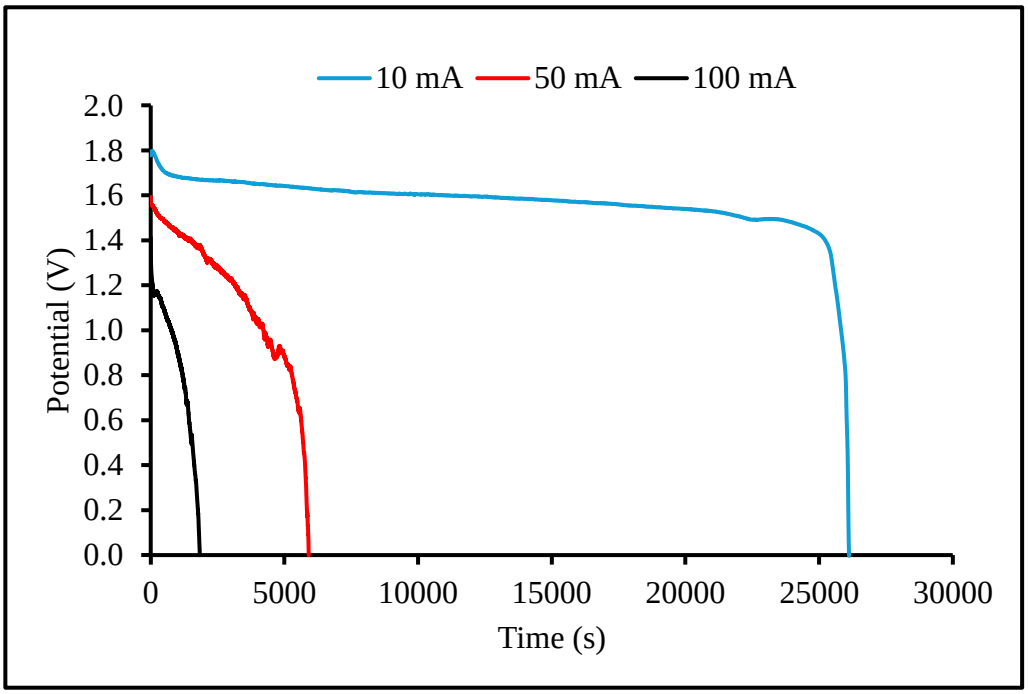

Figure 4.15: Discharge Curve for Al-Air Battery with Gel Electrolyte of 3 M Potassium Hydroxide using Different Discharge Current.

Despite the higher concentration of KOH in the gel electrolyte offer a better electrochemical performance, it accelerates the corrosion of Aluminium anode which is undesirable at it reduces the Al-air battery life cycle. According to Figure 4.16, it reveals that the corrosion rate of the gel electrolyte with 1 M is lower at 0.08456 $mg.min^{-1}.cm^{-2}$ as compared to 0.22617 $mg.min^{-1}.cm^{-2}$ and 0.49430 $mg.min^{-1}.cm^{-2}$ for 2 M and 3 M respectively. As more amount of OH^- ions are supplied in the higher concentration, the electrochemical reaction within the Al-air battery are more efficient which increases the corrosion rate of Aluminium anode. This implies the negatively correlation between the corrosion rate of Aluminium anode and the concentration of KOH in the gel electrolyte. Furthermore, the water absorption ability of these gel electrolyte with varying KOH concentration was also investigated. It reveals in Figure 4.17 that the gel electrolyte with 3 M of KOH has the highest water absorption of 37.11% whereas the gel electrolyte with 1 M and 2 M of KOH has a lower water absorption of 18.45% and 28.36% respectively. This is due to the OH^- ions in KOH are naturally hydrophilic and making them have a strong tendency to bind to water molecules and results in the phenomenon of more electrolyte retained especially when the concentration increases. As mentioned above that the shrinkage of the gel electrolyte can affect the battery performance, thus, shrinkage test was also conducted to discover how the concentration of KOH affects the shrinkage of the gel electrolyte. It reveals in Figure 4.18 that gel electrolyte with 1 M KOH has the least shrinkage effect of 44.42% as compared to 55.04% and 73.53%. While limited OH^- ions supply in the gel electrolyte of 1 M KOH reduces the electrochemical performance, it benefits from suffering lesser shrinkage effect. As there are lesser electrolyte occupying the pores in the gel electrolyte, the reduction in the gel electrolyte volume is minimized when the electrolyte evaporates or consumed during discharging.

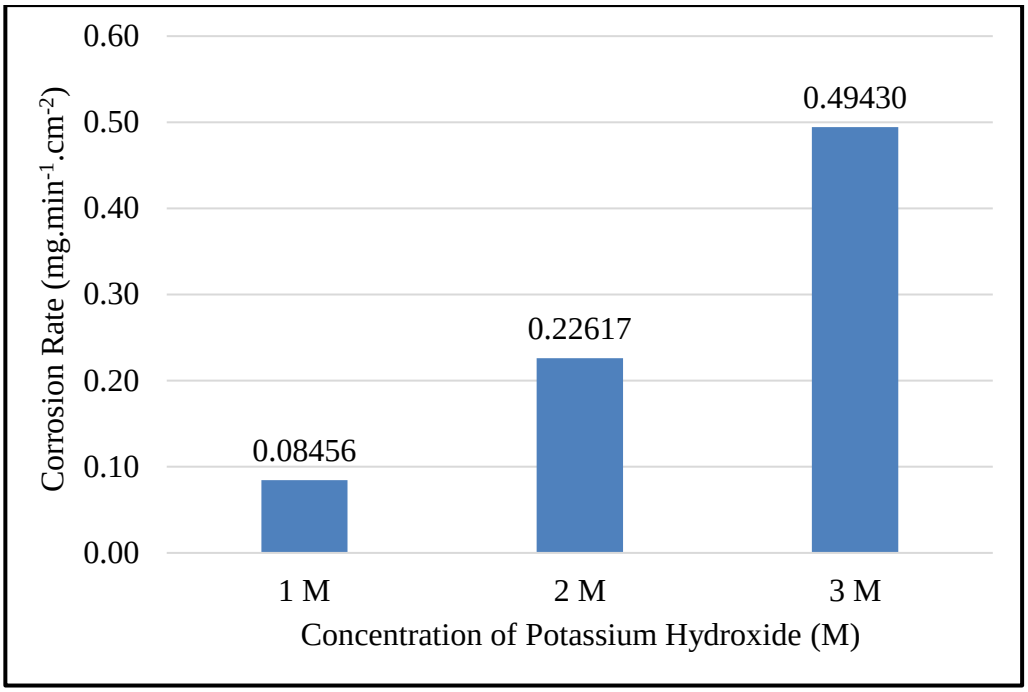

Figure 4.16: Corrosion Rate for Al-air Battery with Gel Electrolyte of Different Concentration of Potassium Hydroxide.

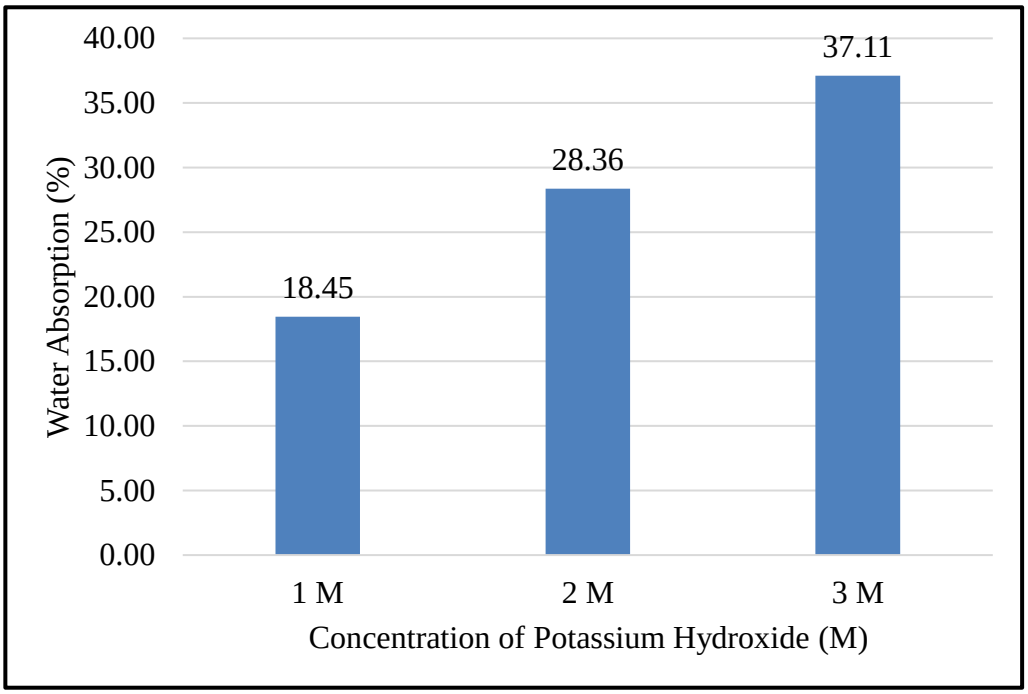

Figure 4.17: Water Absorption for Al-air Battery with Gel Electrolyte of Different Concentration of Potassium Hydroxide.

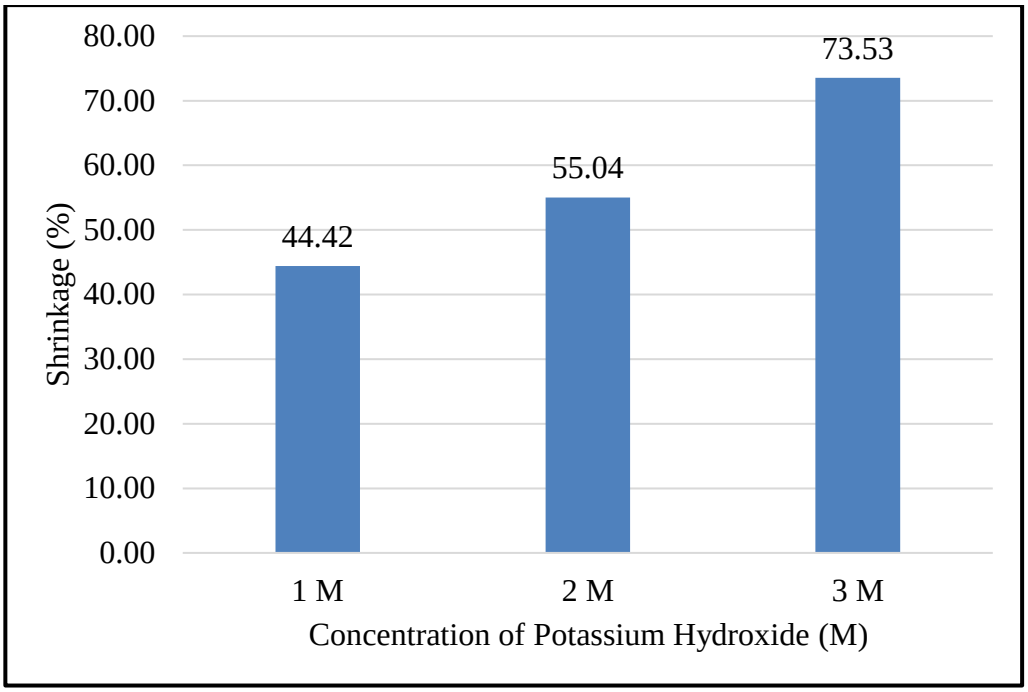

Figure 4.18: Shrinkage for Al-air Battery with Gel Electrolyte of Different Concentration of Potassium Hydroxide.

Table 4.3: Summary of Properties for Gel Electrolyte with Different Concentration of Potassium Hydroxide.

Concentration of Potassium Hydroxide	1 M	2 M	3 M
Open Circuit Voltage (V)	1.86	2.00	1.95
Peak Power Density (mW)	91	100	187
Discharge Time (minutes)	95	192	435
Corrosion Rate ($mg.min^{-1}.cm^{-2}$)	0.08456	0.22617	0.49430
Water Absorption (%)	18.45	28.36	37.11
Shrinkage (%)	44.42	55.04	73.53

The characterization of the surface morphology of the gel electrolyte with 1 M, 2 M and 3 M KOH were done through SEM. The composition of these gel electrolytes remained with 10 wt% of PVA and 10 wt% of NCC content. Therefore, they all have presented the interconnected voids formed by the crosslinking structures due to the incorporation of nanocellulose. Nonetheless, there are slight differences in terms of the pore sizes as they are more darken region in the SEM image as shown in Figure 4.19 for the gel electrolyte with 3 M KOH whereas the gel electrolyte with 1 M KOH reveals a denser region in the gel structure. However, there are no direct relation between the pore sizes in the gel electrolyte structure and the concentration of KOH

added into the gel electrolyte as the increase in KOH concentration primarily affects the OH^- ions supply in the gel electrolyte which affects the ionic conductivity. Among all the gel electrolyte samples, the gel electrolyte fabricated using 3 M KOH presents the best performance of the Al-air battery. When discharging the Al-air battery with thin film cellulose gel electrolyte of 3 M KOH, there are powder formed on the surface of the Aluminium anode and the gel electrolyte due to the electrochemical reactions. However, it is uncertain regarding the content of the powder formed. Therefore, EDAX is performed to identify the compositions of the powder formed from the discharging of the Al-air battery. According to the EDAX pattern as shown in Figure 4.20, the elemental mapping show the presence of Oxygen (O), Aluminium (Al), Carbon (C), Potassium (K) and Sodium (Na). The presence of potassium is contributed from the potassium hydroxide solution. On top of that, the presence of sodium is due to the sodium hydroxide used for nanocellulose dissolution. Overall, It suggests the main component in the powder formed after the discharging test is Aluminium Hydroxide as Aluminium was consumed and reacted with Hydroxide ions.

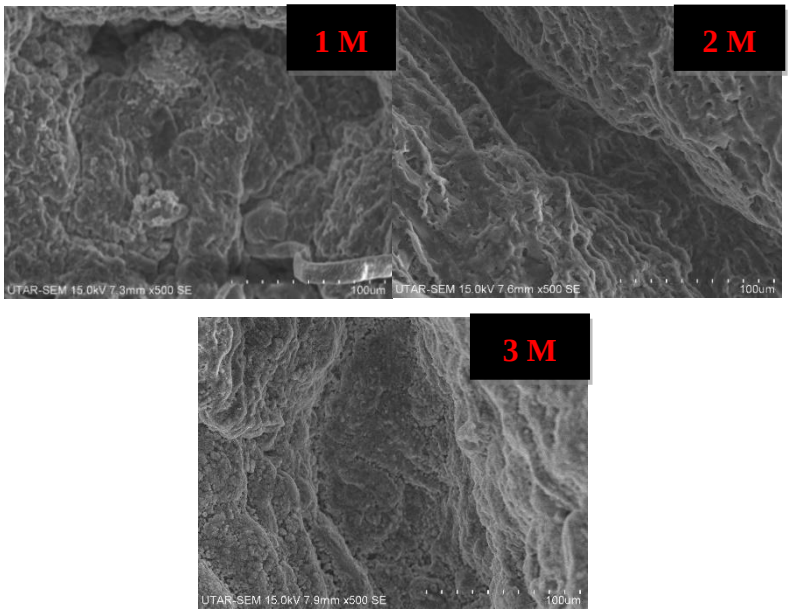

Figure 4.19: SEM Image of 500x magnification of Thin Film Cellulose Gel Electrolyte with 1 M, 2 M and 3 M of Potassium Hydroxide.

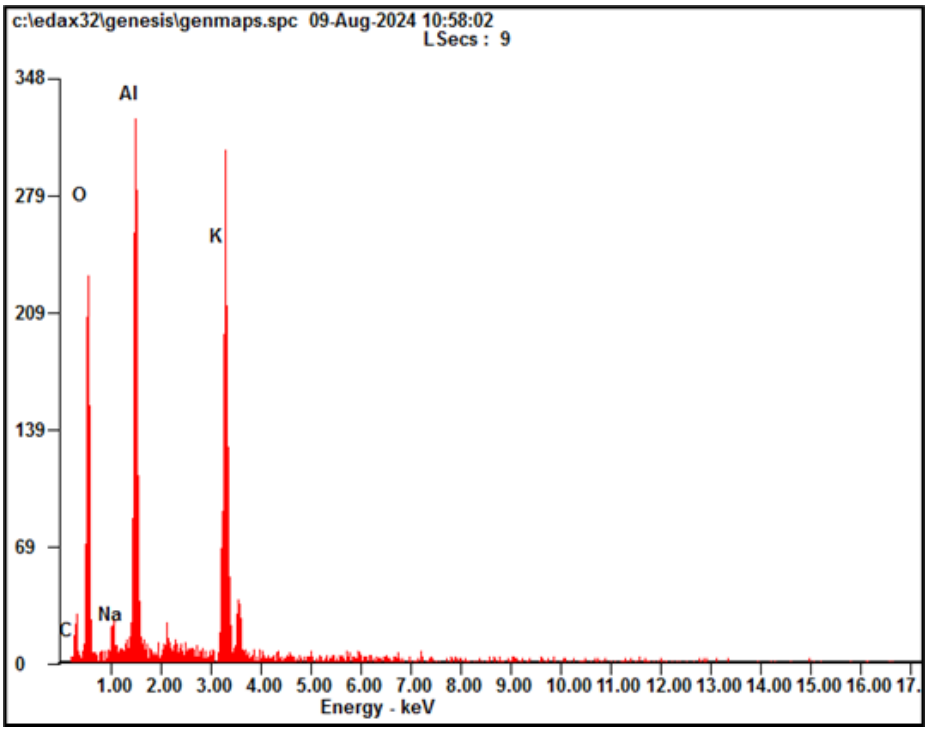

Figure 4.20: EDX Pattern of Bi-Product formed from Discharging of Thin Film Cellulose Gel Electrolyte with 3 M of Potassium Hydroxide.

4.4 Reusability Test

While the electrochemical and discharging performance of an Al-air battery is important, the longevity and stability of the battery is also crucial as the ability to allow a consistent performance when repeatedly used as it is essential for a battery. However, the reusability of the Al-air battery is dependent on the ability of the gel electrolyte to perform consistently over multiple discharge cycles and recharging in terms of electrolyte retention. Hence, reusability test is conducted to determine whether the thin film cellulose gel electrolyte can sustain its electrochemical properties after discharging for several cycles. The thin film cellulose gel electrolyte used in reusability the test is fabricated with the composition of 10 wt% PVA, 10 wt% NCC content with 1 M of KOH and maintained at 20 ml volume of content to allow the better performance according to the justifications as discussed in the above sections. The reusability test is conducted in which after every single set of polarization and discharge test the thin film cellulose gel electrolyte will be immersed in the KOH solution for 1 day before proceeding to the subsequent tests. The Test 1 indicates the test cycle conducted 1 day after the fabrication of the thin film cellulose gel

electrolyte whereas the Test 2 and Test 3 are the test cycles conducted after 2 days and 3 days after the fabrication of the thin film cellulose gel electrolyte. Based on the polarization test results as shown in Figure 4.21, the voltage drop in the low current densities are generally hard to notice as the kinetics of the electrochemical reactions are relatively similar due to the usage of the same air cathode having the similar catalytic activity throughout all the test conducted. However, when moving on to higher current densities in the ohmic region, Test 1 presents a less steep voltage drop as compared to the subsequent Test 2 and Test 3. This suggests that the electrolyte retained within the thin film cellulose gel electrolyte is having the maximum capacity of electrolyte retention which provides surplus of OH^- ions for ion movement and overcome the internal resistance within the battery cell. Furthermore, the voltage drop tends to be significant due to mass transport resulting that the thin film cellulose gel electrolyte can achieve discharger current of 127 mA for Test 1, 92 mA and 60 mA for Test 2 and Test 3 respectively. While cleaning of surface for the thin film cellulose gel electrolyte are done after every test, there could be contaminants or bi-products released during the discharging process occupying the pores in the gel electrolyte. The thin film cellulose gel electrolyte is also prone to experience degradation due to exposing to ambient condition continuously and stored inappropriately. As a result, despite immersing the thin film cellulose gel electrolyte into the KOH solution, the capacity for electrolyte retention is reduced. Hence, the electrochemical performance reduces over time. According to the discharge curve as shown in Figure 4.22, the initial Test 1 was able to maintain 95 minutes of discharging time from 1.6 V to 0 V, but the discharging performance of the Al-air battery shows a significant reduction to 51 minutes for Test 2 and 32 minutes for Test 3. This concludes that the degradation of the gel electrolyte even with the incorporation of nanocellulose is relatively unavoidable. The degradation of gel electrolyte results in suboptimal electrolyte retention, therefore, it cannot facilitate the same amount of OH^- ions as compared to the initial condition and feature the consistency in terms of ions transport. Thus, it results in significant decline in the electrochemical and discharging performance.

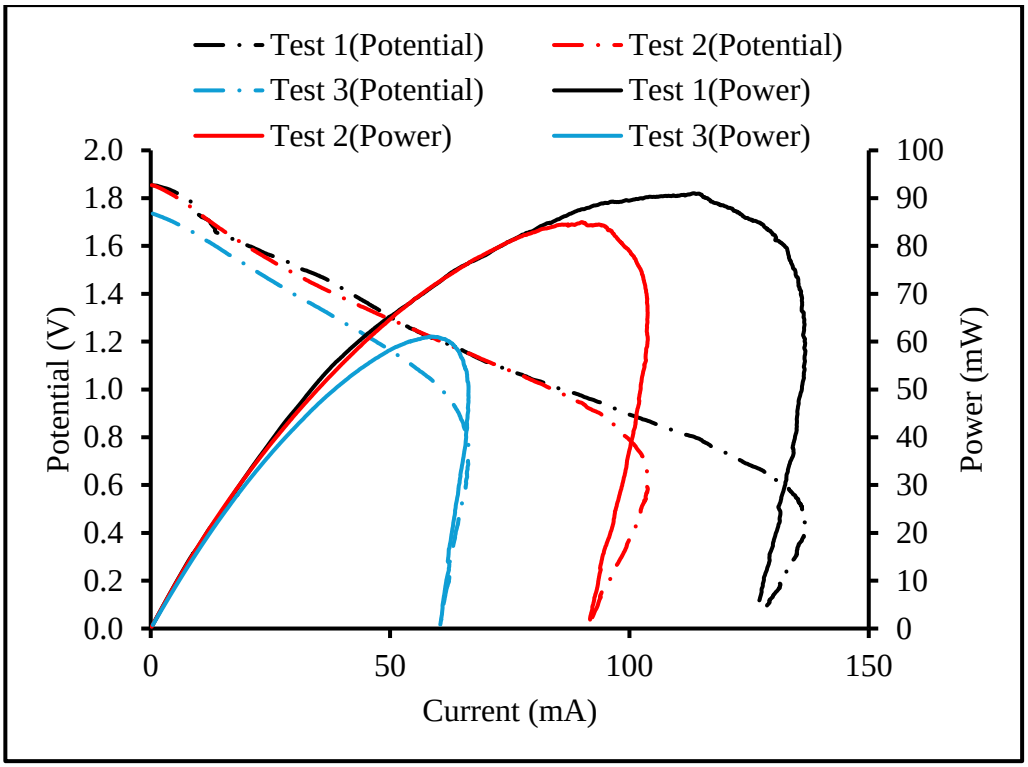

Figure 4.21: Polarization Curve for Al-air Battery with Gel Electrolyte Reused After Days.

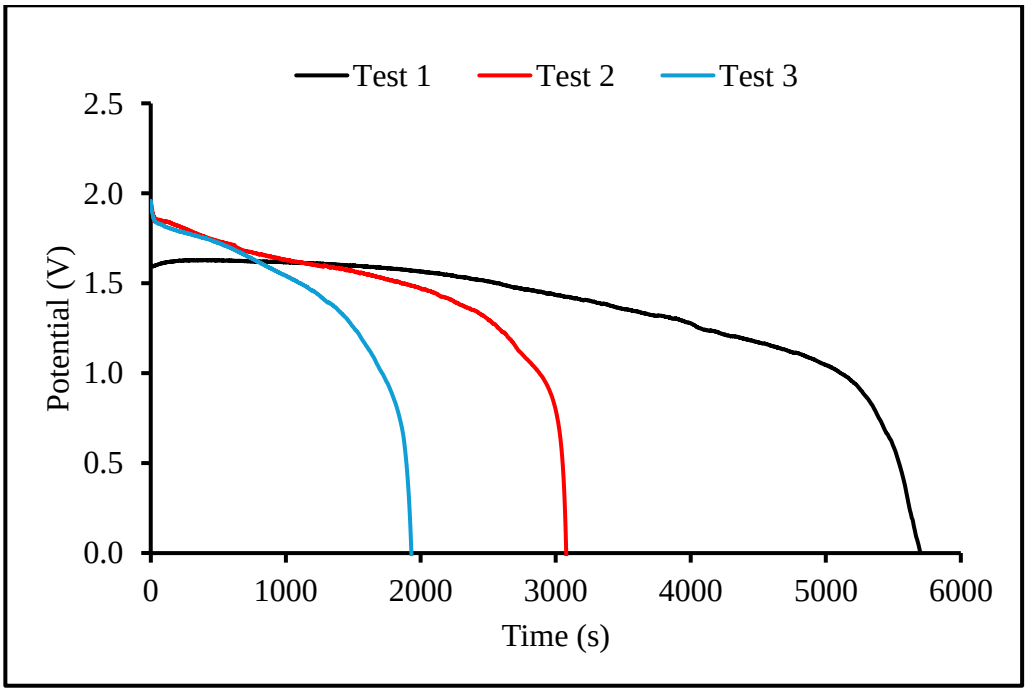

Figure 4.22: Discharge Curve for Al-air Battery with Gel Electrolyte Reused After Days.

4.5 Summary

With the current implementation of Al-air battery technology, the performance of the battery is often associated with factors involving thickness of the gel electrolyte, nanocellulose content incorporated into the gel electrolyte and the concentration of alkaline electrolyte. From the experimental analysis, the results proposed that gel electrolyte with thickness of 20 ml volume content, 10 wt% of NCC content and 3 M of potassium hydroxide generally offers the better electrochemical and discharging performance. The enhanced performance of the Al-air battery is generally due to more porosity form within the gel electrolyte with thicker thickness and the optimum NCC content as well as the surplus of hydroxide ion contributed from higher concentration of KOH within the gel electrolyte. As a result, the electrolyte retention capacity increases along with the ionic conductivity. However, the self-corrosion of Aluminium anode remains to be a major hindrance as a drawback for the better performance of the Al-air battery. Furthermore, the gel electrolyte with a better water absorption ability tends to have a lower shrinkage effect as it can deliberate the evaporation process of the KOH in the gel electrolyte. Despite the superior performance of the thin film cellulose gel electrolyte, it is prone to experience degradation when stored inappropriately which affects the reusability of the gel electrolyte. However, it can be concluded the incorporation of nanocellulose into the gel electrolyte generally enhances the performance of the Al-air battery.

CHAPTER 5

CONCLUSIONS AND RECOMMENDATIONS

5.1 Conslusions

In this research, several thin film cellulose gel electrolyte are fabricated and incorporated into the Aluminium-air battery and the performances of the batteries are characterized. The thickness of the gel electrolyte, nanocellulose content and concentration of potassium hydroxide are important factors which affects the performance of the Al-air battery. The findings of the study reveals that gel electrolyte with the thickness corresponding to 20 ml of content volume yields better battery performance. Although thicker gel electrolyte may result in higher ionic resistance but the additional electrolyte retention compensates the for this, improving the battery performance. Additionally, the gel electrolyte with 10 wt% NCC content produced the optimum battery performance. A comparison of the performance for Al-air battery incorporating gel electrolyte with and without nanocellulose was conducted, it reveals that the gel electrolyte with nanocellulose outperform the gel electrolyte without nanocellulose achieving peak power density of 91 mW along with discharing time of 95 minutes as compared to 55 mW peak power density and 43 minutes of discharging time for gel electrolyte without nanocellulose. Next, a comparison on the nanocellulose content was also conducted. While incorporation of nanocellulose is helpful in creating more porosity which can increase the electrolyte retention but excessive nanocellulose results in negative impact on the battery performance. Furthermore, the concentration of potassium hydroxide and the performance of Al-air battery have a positive correlation whereby higher concentration of KOH will improve the peak power density and discharging time of the battery. Nonetheless, the thin film cellulose gel electrolyte providing better battery performance is often associated with minimal shrinkage effect along with high water absroptin and high corrosion rate at the aluminium anode. In general, the optimum combination of parameters for the gel electrolyte fabrication is thickness with 20 ml of content volume, 10 wt% NCC content and 3 M of KOH concentration which can produce peak power density of 187 mW with a discharging time of 7 hours.

5.2 Recommendation for future work

While the research conducted has achieved an improvement in the electrochemical and discharging performance for Al-air battery, there are few solutions recommended for future work. Due to the degradation of the thin film cellulose gel electrolyte, it limits the reusability of battery and diminishes the longevity of the battery. Despite the improvement in water retention of the thin film cellulose gel electrolyte, the electrolyte will still evaporate when exposed to ambient condition for a long period of time. It is recommended to add additives such as glycerol in the fabrication of the gel electrolyte as it is able to reduce the evaporation rate of the moisture in the gel electrolyte thereby minimizing the water loss. Furthermore, it is recommended to fabricate the Al-air battery with an enclosed battery case which is able to fit the Al anode, gel electrolyte and air cathode as it can also reduce the evaporation of the electrolyte. Additionally, it is recommended to incorporate corrosion inhibitor into the thin film cellulose gel electrolyte to control or even reduce the self-corrosion of the aluminium anode.

Besides that, it is recommended for future studies to focus on the concentration of PVA as it serve as the binder to form the thin film in gel texture which directly affects the physical, chemical, and electrochemical properties of the gel electrolyte. While there are research describing the practicality of PVA in gel electrolyte but there are limited study on the optimisation for the concentration of PVA. The optimisation of the PVA concentration can help to avoid poor gelation or even formation of gel which are too thick. Another recommendations for improvement is to implement air cathode with hydrophobic properties. The electrolyte retained in the thin film cellulose gel electrolyte will cause the air cathode to be damp which impacts on the performance of the Al-air battery.

REFERENCES

Aisiyah, M.M., Masruri, M. and Srihardyastutie, A., 2020. Crystallinity of nanocellulose isolated from the flower waste of pine tree (pinus merkusii). *IOP Conference Series: Materials Science and Engineering*, [e-journal] 833(1), p. 012003. https://doi.org/10.1088/1757-899x/833/1/012003.

Bernard, J., Chatenet, M. and Dalard, F., 2006. Understanding aluminium behaviour in aqueous alkaline solution using coupled techniques. *Electrochimica Acta*, [e-journal] 52(1), pp. 86–93. https://doi.org/10.1016/j.electacta.2006.03.076.

Byon, H.R., Suntivich, J. and Shao-Horn, Y., 2011. Graphene-based non-noble-metal catalysts for oxygen reduction reaction in acid. *Chemistry of Materials*, [e-journal] 23(15), pp. 3421–3428. https://doi.org/10.1021/cm2000649.

Cao, Y.L. et al., 2003. The mechanism of Oxygen Reduction on MnO_2-Catalyzed Air Cathode in alkaline solution. *Journal of Electroanalytical Chemistry*, [e-journal] 557, pp. 127–134. https://doi.org/10.1016/S0022-0728(03)00355-3.

Chang, C. and Zhang, L., 2011. Cellulose-based hydrogels: Present status and application prospects. *Carbohydrate Polymers*, [e-journal] 84(1), pp. 40–53. https://doi.org/10.1016/j.carbpol.2010.12.023.

Chatterjee, K. et al., 2018. Nitrogen-rich carbon nano-onions for oxygen reduction reaction. *Carbon*, [e-journal] 130, pp. 645–651. https://doi.org/10.1016/j.carbon.2018.01.052.

Cheng, F. et al., 2009. MnO_2-based nanostructures as catalysts for electrochemical oxygen reduction in Alkaline Media. *Chemistry of Materials*, [e-journal] 22(3), pp. 898–905. https://doi.org/10.1021/cm901698s.

Cho, Y.-J. et al., 2015b. Aluminium anode for aluminium–air battery – part I: Influence of Aluminium Purity. *Journal of Power Sources*, [e-journal] 277, pp. 370–378. https://doi.org/10.1016/j.jpowsour.2014.12.026.

Chu, D. and Savinell, R.F., 1991. Experimental data on aluminium dissolution in Koh electrolytes. *Electrochimica Acta*, [e-journal] 36(10), pp. 1631–1638. https://doi.org/10.1016/0013-4686(91)85017-2.

Deng, D. et al., 2012. Iron encapsulated within pod‐like carbon nanotubes for oxygen reduction reaction. *Angewandte Chemie International Edition*, [e-journal] 52(1), pp. 371‐375. https://doi.org/10.1002/anie.201204958.

Ditzel, F.I. et al., 2017. Nanocrystalline cellulose extracted from Pine Wood and Corncob. *Carbohydrate Polymers*, [e-journal] 157, pp. 1577–1585. https://doi.org/10.1016/j.carbpol.2016.11.036.

Doche, M.L. et al., 1999. Electrochemical behaviour of aluminium in concentrated NaOH Solutions. *Corrosion Science*, [e-journal] 41(4), pp. 805–826. https://doi.org/10.1016/S0010-938X(98)00107-3.

Egan, D.R. et al., 2013. Developments in electrode materials and electrolytes for aluminium–air batteries. *Journal of Power Sources*, [e-journal] 236, pp. 293–310. https://doi.org/10.1016/j.jpowsour.2013.01.141.

Fan, L., Lu, H. and Leng, J., 2015. Performance of fine structured aluminium anodes in neutral and alkaline electrolytes for Al-Air Batteries. *Electrochimica Acta*, [e-journal] 165, pp. 22–28. https://doi.org/10.1016/j.electacta.2015.03.002.

Fan, X. et al., 2019. Porous nanocomposite gel polymer electrolyte with high ionic conductivity and superior electrolyte retention capability for long-cycle-life flexible zinc–Air Batteries. *Nano Energy*, [e-journal] 56, pp. 454–462. https://doi.org/10.1016/j.nanoen.2018.11.057.

Ge, X. et al., 2015. Oxygen reduction in alkaline media: From mechanisms to recent advances of catalysts. *ACS Catalysis*, [e-journal] 5(8), pp. 4643–4667. https://doi.org/10.1021/acscatal.5b00524.

Guisao, J.P. and Romero, A.J., 2015. Interaction between Zn^{2+} cations and N-methyl-2-pyrrolidone in ionic liquid-based gel polymer electrolytes for Zn Batteries. *Electrochimica Acta*, [e-journal] 176, pp. 1447–1453. https://doi.org/10.1016/j.electacta.2015.07.132.

Hardwick, L.J. and Bruce, P.G., 2012. The pursuit of rechargeable non-aqueous lithium–oxygen battery cathodes. *Current Opinion in Solid State and Materials Science*, [e-journal] 16(4), pp. 178–185. https://doi.org/10.1016/j.cossms.2012.04.001.

Harting, K., Kunz, U. and Turek, T., 2011. Zinc-air batteries: Prospects and challenges for future improvement. *Zeitschrift für Physikalische Chemie*, [e-journal] 226(2), pp. 151–166. https://doi.org/10.1524/zpch.2012.0152.

Jakob, M. et al., 2022 The strength and stiffness of oriented wood and cellulose-fibre materials: A Review. *Progress in Materials Science*, [e-journal] 125, p. 100916. https://doi.org/10.1016/j.pmatsci.2021.100916.

Kuribayashi, I., 1996. Characterization of composite cellulosic separators for rechargeable lithium-ion batteries. *Journal of Power Sources*, [e-journal] 63(1), pp. 87–91. https://doi.org/10.1016/S0378-7753(96)02450-0.

Lee, K.-K. and Kim, K.-B., 2001. Electrochemical impedance characteristics of pure al and Al–Sn Alloys in NaOH solution. *Corrosion Science*, [e-journal] 43(3), pp. 561–575. https://doi.org/10.1016/S0010-938X(00)00060-3.

Lewandowski, A., 2000. Novel poly(vinyl alcohol)–KOH–H_2O alkaline polymer electrolyte. *Solid State Ionics*, [e-journal] 133(3–4), pp. 265–271. https://doi.org/10.1016/S0167-2738(00)00733-5.

Li, F. and Chen, Z., 2013. Graphene-based materials as Nanocatalysts. *Graphene Chemistry*, [e-journal] pp. 347–369. https://doi.org/10.1002/9781118691281.ch15.

Li, Y. et al., 2016. The role of PTFE in cathode transition layer in aqueous electrolyte Li-air battery. *Electrochimica Acta*, [e-journal] 191, pp. 996–1000. https://doi.org/10.1016/j.electacta.2016.01.143.

Li, Z. et al., 2021. Nanocellulose composite gel with high ionic conductivity and long service life for Flexible Zinc-Air Battery. *Polymer Testing*, [e-journal] 104, p. 107380. https://doi.org/10.1016/j.polymertesting.2021.107380.

Liu, K. et al., 2017. Fe_3C@Fe/N Doped Graphene-Like Carbon Sheets as a Highly Efficient Catalyst in Al-Air Batteries. *Journal of The Electrochemical Society*, [e-journal] 164(6). https://doi.org/10.1149/2.0171706jes.

Liu, Y. et al., 2016. Exploring the nitrogen species of nitrogen doped graphene as electrocatalysts for oxygen reduction reaction in Al–Air Batteries. *International Journal of Hydrogen Energy*, [e-journal] 41(24), pp. 10354–10365. https://doi.org/10.1016/j.ijhydene.2015.10.109.

Liu, Y. et al., 2017. A comprehensive review on recent progress in Aluminium–Air Batteries. *Green Energy & Environment*, [e-journal] 2(3), pp. 246–277. https://doi.org/10.1016/j.gee.2017.06.006.

Ma, G. et al., 2014. High performance solid-state supercapacitor with PVA–KOH–$K_3[Fe(CN)_6]$ gel polymer as electrolyte and separator. *Journal of Power Sources*, [e-journal] 256, pp. 281–287. https://doi.org/10.1016/j.jpowsour.2014.01.062.

Ma, J. et al., 2013. Electrochemical polarization and corrosion behavior of Al–Zn–in based alloy in acidity and alkalinity solutions. *International Journal of Hydrogen Energy*, [e-journal] 38(34), pp. 14896–14902. https://doi.org/10.1016/j.ijhydene.2013.09.046.

Ma, J. et al., 2014. Performance of Al−1Mg−1Zn−0.1Ga−0.1Sn as anode for Al-Air Battery. *Electrochimica Acta*, [e-journal] 129, pp. 69–75. https://doi.org/10.1016/j.electacta.2014.02.080.

Ma, J., Wen, J., Li, Q. and Zhang, Q., 2013. Effects of acidity and alkalinity on corrosion behaviour of Al–Zn–Mg based anode alloy. *Journal of Power Sources*, [e-journal] 226, pp. 156–161. https://doi.org/10.1016/j.jpowsour.2012.10.075.

Mamtani, K. et al., 2018. Insights into oxygen reduction reaction (ORR) and oxygen evolution reaction (OER) active sites for nitrogen-doped carbon

nanostructures (CN_X) in Acidic Media. *Applied Catalysis B: Environmental*, [e-journal] 220, pp. 88–97. https://doi.org/10.1016/j.apcatb.2017.07.086.

Mohamad, A.A., 2008. Electrochemical properties of aluminium anodes in gel electrolyte-based aluminium-air batteries. *Corrosion Science*, [e-journal] 50(12), pp. 3475–3479. https://doi.org/10.1016/j.corsci.2008.09.001.

Mokhtar, M. et al., 2015. Recent developments in materials for aluminium–air batteries: A Review. *Journal of Industrial and Engineering Chemistry*, [e-journal] 32, pp. 1–20. https://doi.org/10.1016/j.jiec.2015.08.004.

Moon, R.J. et al., 2011. Cellulose nanomaterials review: Structure, properties and nanocomposites. *Chemical Society Reviews*, [e-journal] 40(7), p. 3941. http://dx.doi.org/10.1039/c0cs00108b.

Mutlu, R.N. and Yazıcı, B., 2018. Copper-deposited aluminium anode for aluminium-air battery. *Journal of Solid State Electrochemistry*, [e-journal] 23(2), pp. 529–541. https://doi.org/10.1007/s10008-018-4146-1.

Nada, A.A. et al., 2023. Ionic conductive cellulose-based hydrogels for al-air batteries: Influence of the charged-functional groups on the electrochemical properties. *Journal of Power Sources*, [e-journal] 572, p. 233089. https://doi.org/10.1016/j.jpowsour.2023.233089.

Nestoridi, M. et al., 2008. The study of aluminium anodes for high power density al/air batteries with brine electrolytes. *Journal of Power Sources*, [e-journal] 178(1), pp. 445–455. https://doi.org/10.1016/j.jpowsour.2007.11.108.

Olabi, A.G. et al., 2021. Metal-air batteries—A Review. *Energies*, [e-journal] 14(21), p. 7373. https://doi.org/10.3390/en14217373.

Park, I.-J., Choi, S.-R. and Kim, J.-G., 2017. Aluminium anode for aluminium-air battery – part II: Influence of in addition on the electrochemical characteristics of Al-Zn alloy in Alkaline Solution. *Journal of Power Sources*, [e-journal] 357, pp. 47–55. https://doi.org/10.1016/j.jpowsour.2017.04.097.

Parsons, R., 1967. Atlas of Electrochemical Equilibria in aqueous solutions. *Journal of Electroanalytical Chemistry and Interfacial Electrochemistry*, [e-journal] 13(4), p. 471. https://doi.org/10.1016/0022-0728(67)80059-7.

Pino, M. et al., 2015. Performance of commercial aluminium alloys as anodes in gelled electrolyte aluminium-air batteries. *Journal of Power Sources*, [e-journal] 299, pp. 195–201. https://doi.org/10.1016/j.jpowsour.2015.08.088.

Qu, S. et al., 2017. Electrochemical approach to prepare integrated air electrodes for highly stretchable zinc-air battery array with tunable output voltage and current for wearable electronics. *Nano Energy*, [e-journal] 39, pp. 101–110. https://doi.org/10.1016/j.nanoen.2017.06.045.

Rahman, Md.A., Wang, X. and Wen, C., 2013. High energy density metal-air batteries: A Review. *Journal of The Electrochemical Society*, [e-journal] 160(10). https://doi.org/10.1149/2.062310jes.

Roche, I. et al., 2006. Carbon-supported manganese oxide nanoparticles as electrocatalysts for the oxygen reduction reaction (ORR) in alkaline medium: physical characterizations and Orr Mechanism. *The Journal of Physical Chemistry C*, [e-journal] 111(3), pp. 1434–1443. https://doi.org/10.1021/jp0647986.

Santos, D.M., Sequeira, C.A. and Figueiredo, J.L., 2013. Hydrogen production by alkaline water electrolysis. *Química Nova*, [e-journal] 36(8), pp. 1176–1193. https://doi.org/10.1590/S0100-40422013000800017.

Santos, F. et al., 2019. Structural modifications and Ionic transport of PVA-KOH Hydrogels applied in Zn/Air Batteries. *Journal of Electroanalytical Chemistry*, [e-journal] 850, p. 113380. https://doi.org/10.1016/j.jelechem.2019.113380.

Selan, A.A. et al., 2023. Preliminary analysis of the cellulose-based battery separator. *Materials Today: Proceedings*, [e-journal] https://doi.org/10.1016/j.matpr.2023.01.294.

Shen, J. et al., 2018. Preparation of Co–N carbon nanosheet oxygen electrode catalyst by controlled crystallization of cobalt salt precursors for all-solid-state Al–Air Battery. *RSC Advances*, [e-journal] 8(39), pp. 22193–22198. https://doi.org/10.1039/C8RA03245A.

Sun, Z. and Lu, H., 2015. Performance of Al-0.5In as anode for Al–Air Battery in inhibited alkaline solutions. *Journal of The Electrochemical Society*, [e-journal] 162(8). https://doi.org/10.1149/2.0881508jes.

Sun, Z. et al., 2015. Performance of Al-Air batteries based on Al–Ga, Al–In and Al–Sn alloy electrodes. *Journal of The Electrochemical Society*, [e-journal] 162(10). https://doi.org/10.1149/2.0681510jes.

Tran, T.N., Chung, H.-J. and Ivey, D.G., 2019. A study of alkaline gel polymer electrolytes for rechargeable Zinc–Air Batteries. *Electrochimica Acta*, [e-journal] 327, p. 135021. https://doi.org/10.1016/j.electacta.2019.135021.

Tuck, C.D., Hunter, J.A. and Scamans, G.M., 1987. The electrochemical behavior of Al-Ga alloys in alkaline and neutral electrolytes. *Journal of The Electrochemical Society*, [e-journal] 134(12), pp. 2970–2981. https://doi.org/10.1149/1.2100325.

Wang, C. et al., 2008. A general approach to the size- and shape-controlled synthesis of platinum nanoparticles and their catalytic reduction of oxygen. *Angewandte Chemie International Edition*, [e-journal] 47(19), pp. 3588–3591. https://doi.org/10.1002/anie.200800073.

Wang, L. et al., 2013. A hybrid aluminium/hydrogen/air cell system. *International Journal of Hydrogen Energy*, [e-journal] 38(34), pp. 14801–14809. https://doi.org/10.1016/j.ijhydene.2013.09.036.

Wang, Q. et al., 2017. Performances of an Al–0.15 Bi–0.15 Pb–0.035 Ga alloy as an anode for Al–Air Batteries in neutral and alkaline electrolytes. *RSC Advances*, [e-journal] 7(42), pp. 25838–25847. https://doi.org/10.1039/C7RA02918G.

Wang, S., Lu, A. and Zhang, L., 2016. Recent advances in regenerated cellulose materials. *Progress in Polymer Science*, [e-journal] 53, pp. 169–206. https://doi.org/10.1016/j.progpolymsci.2015.07.003.

Wang, Y. et al., 2019. Parametric study and optimization of a low-cost paper-based Al-air battery with corrosion inhibition ability. *Applied Energy*, [e-journal] 251, p. 113342. https://doi.org/10.1016/j.apenergy.2019.113342.

Wilhelmsen, W. et al., 1991. The electrochemical behaviour of Al-In alloys in alkaline electrolytes. *Electrochimica Acta*, [e-journal] 36(1), pp. 79 – 85. https://doi.org/10.1016/0013-4686(91)85182-7.

Xia, L. et al., 2015. Flexible SnO_2/N-doped carbon nanofiber films as integrated electrodes for lithium-ion batteries with superior rate capacity and long cycle life. *Small*, [e-journal] 12(7), pp. 853–859. https://doi.org/10.1002/smll.201503315.

Yang, C.-C. and Lin, S.-J., 2002. Preparation of composite alkaline polymer electrolyte. *Materials Letters*, [e-journal] 57(4), pp. 873–881. https://doi.org/10.1016/S0167-577X(02)00888-1.

Yang, S., 2002. Design and analysis of aluminium/air battery system for electric vehicles. *Journal of Power Sources*, [e-journal] 112(1), pp. 162–173. https://doi.org/10.1016/S0378-7753(02)00370-1.

Zhong, G. et al., 2015. Nitrogen doped carbon nanotubes with encapsulated ferric carbide as excellent electrocatalyst for oxygen reduction reaction in acid and alkaline media. *Journal of Power Sources*, [e-journal] 286, pp. 495–503. https://doi.org/10.1016/j.jpowsour.2015.04.021.

Zhu, M. et al., 2016. High performance and biodegradable skeleton material based on soy protein isolate for gel polymer electrolyte. ACS *Sustainable Chemistry & Engineering*, [e-journal] 4(9), pp. 4498–4505. https://doi.org/10.1021/acssuschemeng.6b01218.

Zuo, Y. et al., 2020. Electrospun Al_2O_3 film as inhibiting corrosion interlayer of anode for solid aluminium–Air Batteries. *Batteries*, [e-journal] 6(1), p. 19. https://doi.org/10.3390/batteries6010019.